Hunting for the second Higgs resonance at LHC

Maurizio Consoli

INFN, Sezione di Catania, Italy

Les Rencontres de Physique de la Vallée d'Aoste, March 2023

References:

M.C., L.Cosmai, Int. J. Mod. Phys. **A35** (2020) 2050103; hep-ph/2006.15378

M.C., L.Cosmai, Symmetry **12** (2020) 2037; doi:103390/sym12122037

M.C. , in Veltman Memorial Volume, Acta Phys. Pol. **B52** (2021) 763; hep-ph/2106.06543

M.C., L.Cosmai, Int. J. Mod. Phys. **A37** (2022) 2250091; arXiv:2111.08962v2 [hep-ph]

M.C., L.Cosmai, F. Fabbri, arXiv:2208.00920v2 [hep-ph], revised December 2022

M.C., L.Cosmai, F.Fabbri, Universe **9** (2023) 99; MDPI Special Issue: Higgs and BSM Physics

Abstract

1) Beside the resonance with m_h=125 GeV, theoretical arguments + lattice simulations suggest a **second Higgs resonance** with **$(M_H)^{Theor} \approx$ 690(22) GeV** and **$(\Gamma_H)^{Theor} \approx$ 30÷40 GeV** (decaying predominantly to **$t\bar{t}$** quarks) mainly produced at LHC by gluon-gluon Fusion. Being (presently) impossible to detect the signal in the **$t\,\bar{t}$** channel, we have considered other final states:

2) ATLAS charged 4-lepton events indicate a +**2.5 σ** excess at 680(30) GeV followed by –**3.3 σ** defect at 740(30) GeV→ Breit-Wigner peak followed by negative (M^2–s) interference with a resonance of mass **$(M_H)^{EXP} \approx$ 700 GeV**

3) Furthermore:

i) ATLAS high-mass γγ events → + **3.3 σ** at 684 (16) GeV

ii) ATLAS ($b\bar{b}$+γγ) channel → + **1.2 σ** at 650 (25) GeV

iii) CMS ($b\bar{b}$+γγ) channel → + **1.6 σ** at 675 (25) GeV

(ii + iii) **Combined ≈ 2 σ**

iv) CMS γγ produced in pp double-diffractive scattering→ **3.0 σ** at 650(40) GeV

4) From the alignment of the mass values with the theoretical prediction → **local significance should NOT be downgraded by the "look-elsewhere" effect**

5) The negligible correlation of the data gives a cumulated probability at (above) the traditional 5 σ level. **Instability:** watch 2 crucial missing sets of RUN2 data

Presently accepted view: the mass spectrum of the Higgs field consists of a **single narrow resonance** of mass **m_h = 125 GeV**

At present, the excitation spectrum of the Higgs field is described in terms of a single narrow resonance of mass $m_h = 125$ GeV associated with the quadratic shape of the effective potential at its minimum. In a description of Spontaneous Symmetry Breaking (SSB) as a second-order phase transition, this point of view is well summarized in the review of the Particle Data Group [1] where the scalar potential is expressed as

$$V_{\rm PDG}(\varphi) = -\frac{1}{2}m^2_{\rm PDG}\varphi^2 + \frac{1}{4}\lambda_{\rm PDG}\varphi^4 \qquad (1)$$

By fixing $m_{\rm PDG} \sim 88.8$ GeV and $\lambda_{\rm PDG} \sim 0.13$, this has a minimum at $|\varphi| = \langle\Phi\rangle \sim 246$ GeV and a second derivative $V''_{\rm PDG}(\langle\Phi\rangle) \equiv m_h^2 = (125\ {\rm GeV})^2$.

- In this talk, I will discuss the possibility of a richer mass spectrum for the Higgs field

- Actually, I have now discovered that, before our work, this idea had already been considered by van der Bij

Vol. 11 (2018) *Acta Physica Polonica B Proceedings Supplement* No 2

PHYSICS AFTER THE DISCOVERY OF THE HIGGS BOSON*

J.J. van der Bij

Institut für Physik, Albert-Ludwigs-Universität Freiburg, Germany

- About the Higgs propagator:

«This said, the real reason we need the Higgs field is renormalizability. **This, however, does not imply that one must have a single Higgs particle peak.** Fundamental quantum field theory tells us only that the Higgs field must have a Källén–Lehmann spectral density [14,15]. This density can be largely arbitrary, but must fall off fast enough at infinity, because otherwise the theory is not renormalizable. **Since in some sense the Higgs field is considered to be different from the other fields**, it is not unreasonable to expect a non-trivial density. The premier scientific goal regarding electroweak symmetry breaking is thus to measure the Källén–Lehmann spectral density of the Higgs propagator**».**

(After this, van der Bij considers the case of a Higgs propagator with 2 peaks where indeed the spectral density vanishes fast enough at infinity. Subtleties for radiative corrections)

The mass scales in the effective potential

- In general, in the effective potential, there are TWO possible mass scales:

a) $\mathbf{(m_h)^2 = V''_{eff}(\langle\Phi\rangle) = G^{-1}(p=0)}$. It gives the quadratic shape of the potential (the inverse zero-momentum propagator). Through $\mathbf{(m_h)^2/\langle\Phi\rangle^2 \approx \lambda_{PDG}}$ it also fixes the interactions among the fluctuations of the broken-symmetry phase)

b) $\mathbf{M_H}$ which measures the Zero-Point Energy (*ZPE*) entering the potential depth.

On the other hand, the zero-point energy is (one-half of) the trace of the logarithm of the inverse propagator $G^{-1}(p) = (p^2 - \Pi(p))$. Therefore, after subtracting constant terms and quadratic divergences, matching the 1-loop zero-point energy("ZPE") gives the relation

$$ZPE \sim -\frac{1}{4}\int_{p_{\rm min}}^{p_{\rm max}} \frac{d^4p}{(2\pi)^4}\frac{\Pi^2(p)}{p^4} \sim -\frac{\langle\Pi^2(p)\rangle}{64\pi^2}\ln\frac{p^2_{\rm max}}{p^2_{\rm min}} \sim -\frac{M_H^4}{64\pi^2}\ln\frac{\Lambda_s^2}{M_H^2} \qquad (1)$$

Thus M_H^2 effectively includes all momenta by reflecting an average $|\langle\Pi(p)\rangle|$ at larger p^2.

The coupling λ_{PDG}

- $\lambda_{PDG} = \lambda(\mu = \langle\Phi\rangle)$ is the scalar self-coupling at the Fermi scale
- Within the «Triviality» of Φ^4 theories in 4D, it depends on the ultraviolet cutoff Λ of the scalar sector (the Landau pole) i.e. $\lambda_{PDG} \approx L^{-1}$ with $L \approx \ln(\Lambda/\langle\Phi\rangle)$

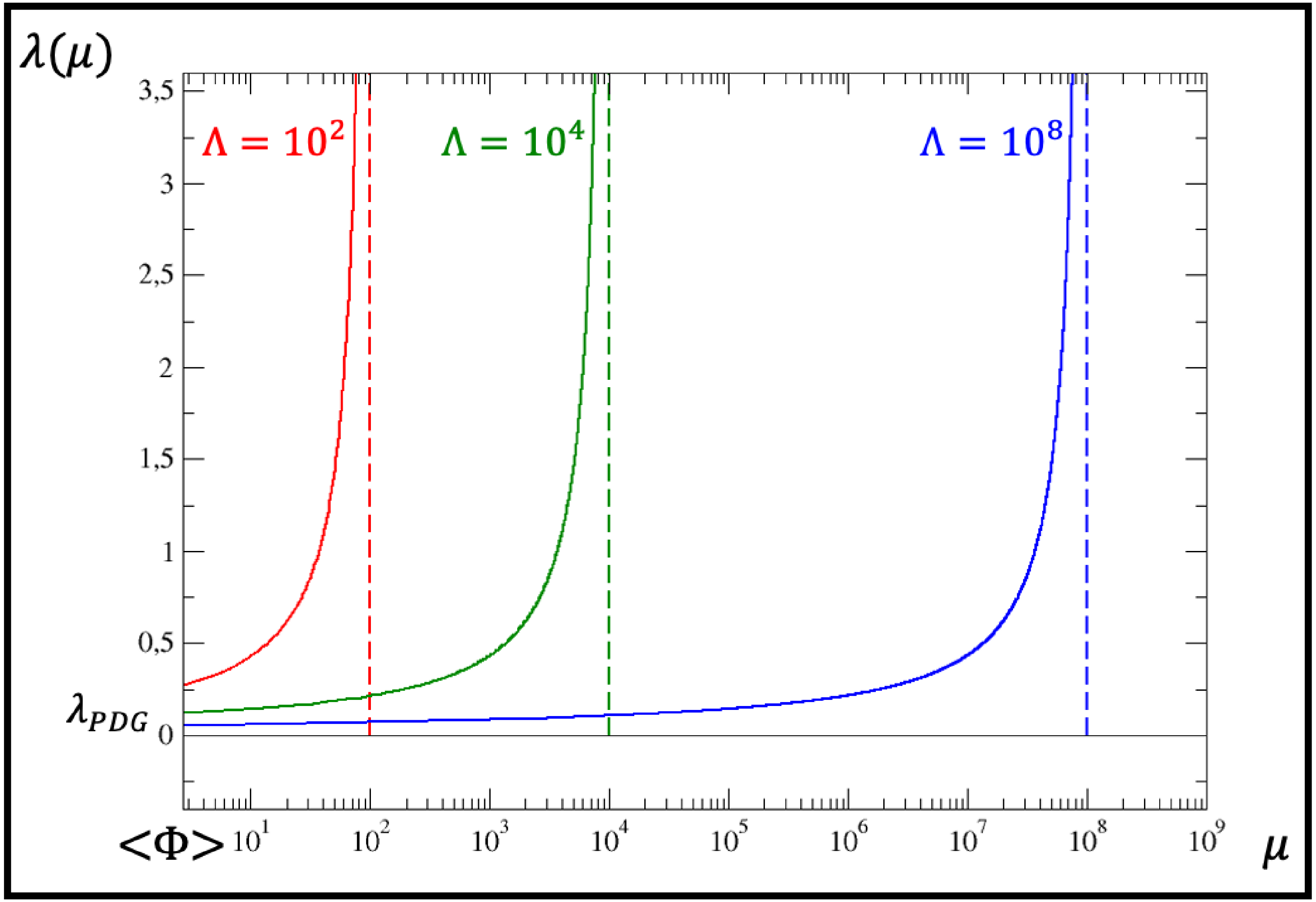

Perturbative view

- In standard perturbation theory the two mass scales are very close

$$\mathbf{M_H = m_h\ [1 + O\ (\lambda_{PDG})]\ \approx\ m_h}$$

- Only one mass scale in the continuum limit where $\boldsymbol{\lambda_{PDG} \approx L^{-1}} \rightarrow 0$

- However, by changing the description of SSB, $\mathbf{M_H}$ can be much larger than $\mathbf{m_h}$

- The Higgs field determines the vacuum of the Standard Model
- This vacuum is not just a trivial emptiness: «What we experience as empty space is nothing but the configuration of the Higgs field with the lowest possible energy. If we move from field jargon to particle jargon, this means that empty space is actually filled by the quanta of the Higgs field. They have Bose condensed»

(G. ‘t Hooft, Search of the Ultimate Building Blocks, 1997)

- But Bose condensation of what? Fully understanding the instability of the symmetric phase requires to improve on the usual «tachyonic» picture of the $\langle\Phi\rangle = 0$ vacuum based on a second-order phase transition
- Replacing second-order phase transition with (weak) first-order phase transition, there is **no negative quadratic mass in the classical potential**
- **ZPE are much larger because they have to induce SSB →** Motivations for a second resonance of the Higgs field

SSB in cutoff Φ^4 is a (weak) first-order phase transition (NOT second-order as with $V_{PDG}(\varphi)$)

- In the standard picture (classical double-well potential with perturbative quantum correction) SSB is a 2nd-order phase transition. Is this so obvious?
- For instance, in the presence of gauge bosons, SSB is a (weak) first-order phase transition→ the Coleman-Weinberg massless limit corresponds to the broken phase. What about the **cutoff version** of pure Φ^4 (in 4D)?
- Lattice simulations of **pure Φ^4** also give a (weak) 1st order phase transition
- Magnetization as function of temperature

→ From Akiyama et al. PRD 100(2019)0545

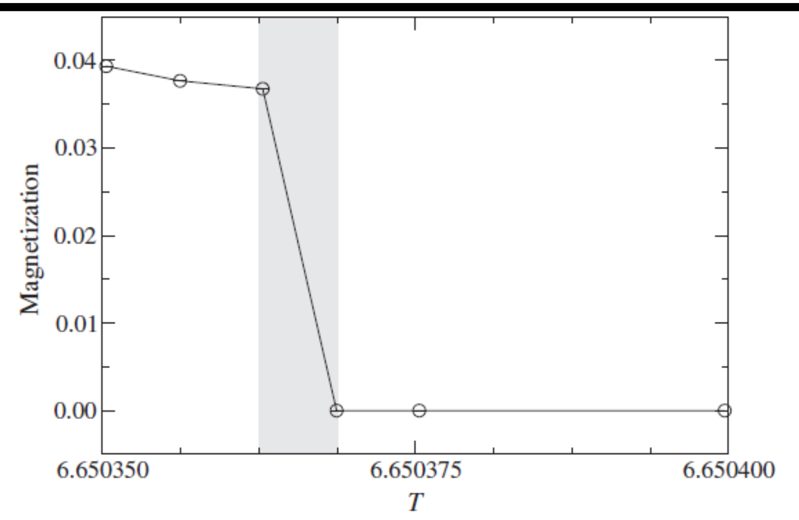

FIG. 7. Spontaneous magnetization in the thermodynamic limit with $D_{cut} = 13$. Error bars, provided by extrapolation, are within symbols. $T_c(D_{cut} = 13)$ estimated by $X^{(n)}$ of Eq. (15) is within the gray band.

Known approximations to $\mathbf{V_{eff}(\varphi)}$ where **SSB is a weak first-order phase transition → 2 distinct mass scales**

- In **known** approximations where SSB is weakly first-order: $\mathbf{m_h}$ (from quadratic shape) and $\mathbf{M_H}$ (from *ZPE*) do NOT scale uniformly with $\mathbf{L \approx \ln(\Lambda/\langle\Phi\rangle)}$

- This is because $\mathbf{M_H}$ sets the ground-state energy which is a RG-invariant quantity. Therefore → $\mathbf{M_H}$ = **Λ-independent**:

$$(\mathbf{M_H})^2 = \mathbf{K}^2 \langle\mathbf{\Phi}\rangle^2 \qquad \text{whereas} \qquad (\mathbf{m_h})^2 \approx \mathbf{L}^{-1} \langle\mathbf{\Phi}\rangle^2 \ll (\mathbf{M_H})^2$$

- Again, as in perturbation theory, only one mass scale when $\Lambda \to \infty$. However, now $\mathbf{M_H}$ and $\mathbf{m_h}$ can be very different in the cutoff theory.
- **IMPORTANT:** Vacuum stability depends on the large $\mathbf{M_H}$ and NOT on $\mathbf{m_h}$. SSB could be induced in the pure scalar sector regardless of M_W, M_Z, $m_{top.}$
- Still m_h fixes the quadratic shape of the potential and the interaction of the fluctuations in the broken-symmetry phase → **$\mathbf{M_H}$ is not a measure of observable interactions**

- If $\mathbf{M_H} \neq \mathbf{m_h}$ → propagator **G (p)** has NOT a single-pole structure

- Check: perform **lattice simulations of G(p)**

- Extract $\mathbf{m_h}$ **from G(p)** when p→0 and $\mathbf{M_H}$ from **G(p)** at larger (Euclidean) momenta

- Check the expected logarithmic scaling law

$$(\mathbf{M_H})^2 \approx \quad \mathbf{L}\,(\mathbf{m_h})^2$$

Stevenson's study of the lattice propagator: NPB729(2005)542

(data from Balog, Duncan, Willey, Niedermeyer, Weisz: NPB714(2005)256)

Stevenson fits the lattice data and reports the **rescaled** propagator data.

$$\zeta \equiv (\hat{p}^2 + m^2)G(p)$$

Standard one-pole propagator → ζ has a flat profile

Left: re-scaling with the mass 0.1691 from the p=0 limit
Right: re-scaling with the mass giving a flat profile at larger p^2

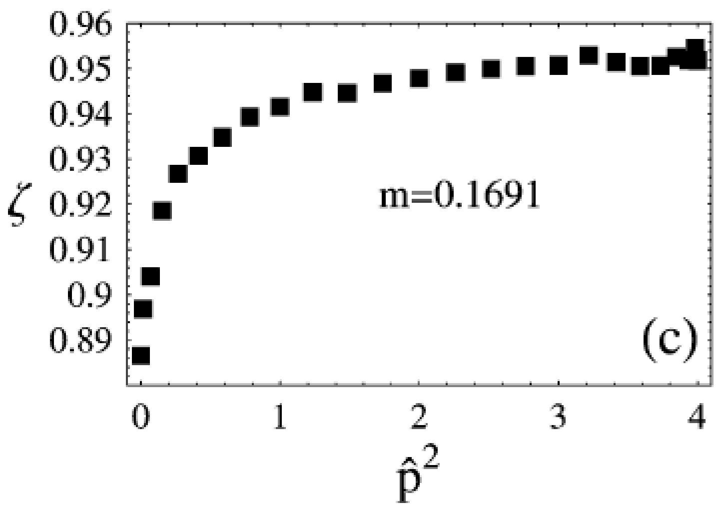

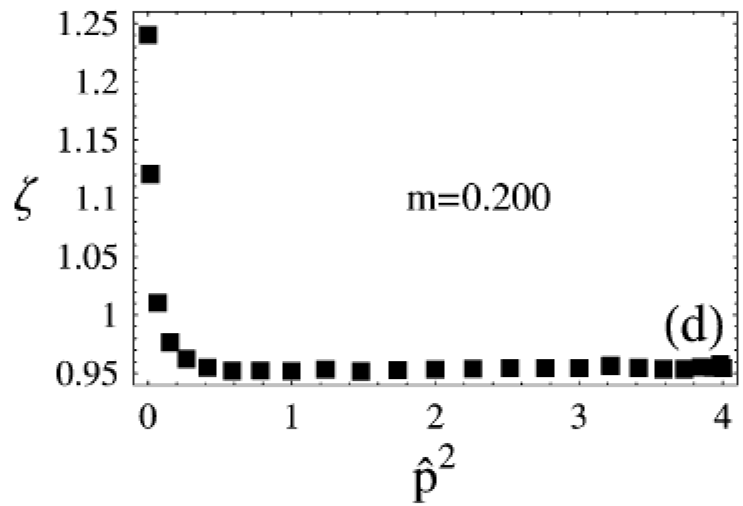

Lattice consistency checks

(M.C. and Leonardo Cosmai, Int. J. Mod. Phys. A35 (2020) 2050103; hep-ph/2006.15378

- A consistency check: no two-mass structure in the symmetric phase. Plot the re-scaled propagator. **Single mass → straight line**

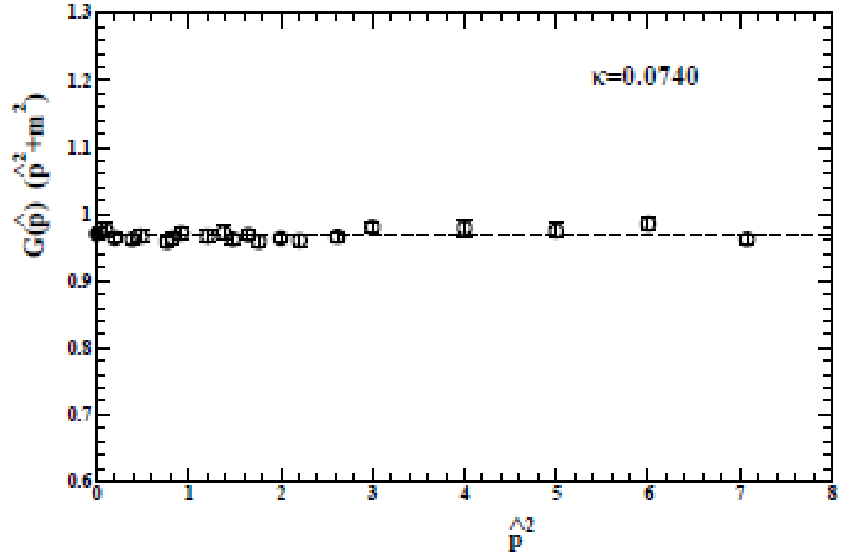

Figure 1: *The lattice data of ref.[8] for the re-scaled propagator in the symmetric phase at* $\kappa = 0.074$ *as a function of the square lattice momentum* $\hat{p}^2$. *The fitted mass from high* $\hat{p}^2$, $m_{\rm latt} = 0.2141(28)$, *describes well the data down to* $\hat{p} = 0$. *The dashed line indicates the value of* $Z_{\rm prop} = 0.9682(23)$ *and the* $\hat{p} = 0$ *point is* $2\kappa\chi m^2_{\rm latt} = 0.9702(91)$.

Propagator on a 76^4 lattice: 2 flat ranges→ 2 mass-shell regions

(M.C. and L.Cosmai, IJMP A35 (2020) 2050103; hep-ph/2006.15378

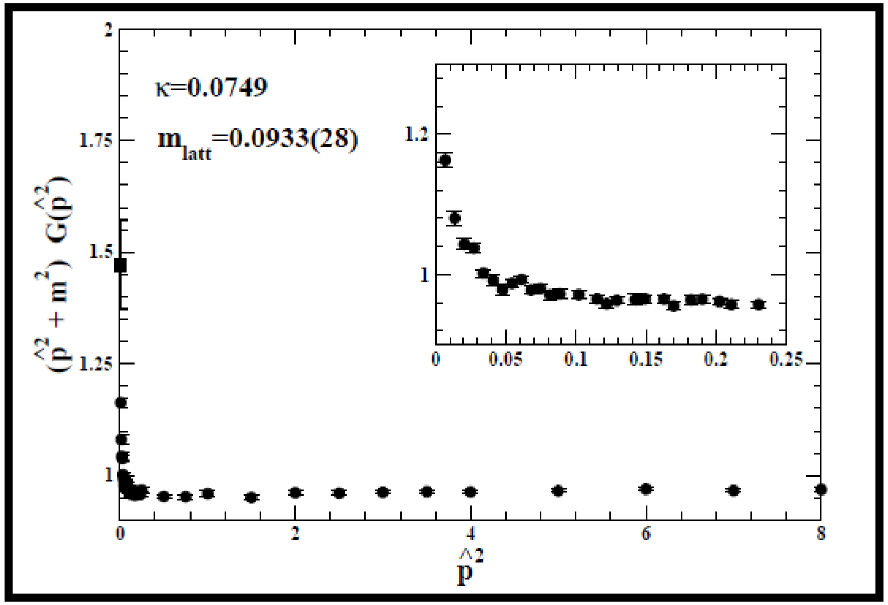

Figure 2: *The propagator data of ref.[8], for* $\kappa = 0.0749$*, rescaled with the lattice mass* $M_H \equiv m_{\rm latt} = 0.0933(28)$ *obtained from the fit to all data with* $\hat{p}^2 > 0.1$*. The peak at* $p = 0$ *is* $M_H^2/m_h^2 = 1.47(9)$ *as computed from the fitted* M_H *and* $m_h = (2\kappa\chi)^{-1/2} = 0.0769(8)$.

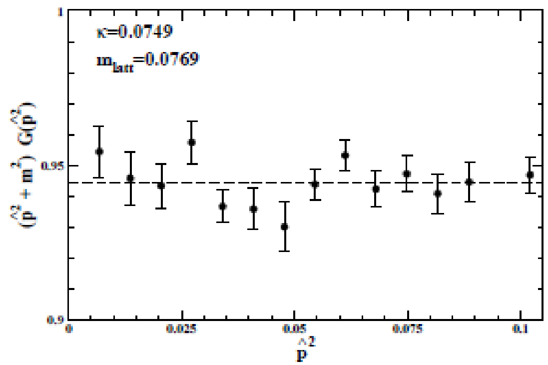

Figure 3: *The propagator data of ref.[8] at* $\kappa = 0.0749$ *for* $\hat{p}^2 < 0.1$*. The lattice mass used here for the rescaling was fixed at the value* $m_h = (2\kappa\chi)^{-1/2} = 0.0769(8)$.

Two-mass structure of the lattice propagator

(same structure as van der Bij's propagator but different motivations)

By computing m_h^2 from the $p \to 0$ limit of $G(p)$ and M_H^2 from its behaviour at higher p^2, the lattice data are consistent with a transition between two different regimes. By analogy with superfluid He-4, where the observed energy spectrum arises by combining the two quasi-particle spectra of phonons and rotons, the lattice data were well described in the full momentum region by the model form [7]

$$G(p) \sim \frac{1 - I(p)}{2} \frac{1}{p^2 + m_h^2} + \frac{1 + I(p)}{2} \frac{1}{p^2 + M_h^2} \tag{4}$$

with an interpolating function $I(p)$ which depends on an intermediate momentum scale p_0 and tends to $+1$ for large $p^2 \gg p_0^2$ and to -1 when $p^2 \to 0$. Most notably, the lattice data were also consistent with the expected increasing logarithmic trend $M_H^2 \sim L m_h^2$ when approaching the continuum limit [3].

Phenomenological implications

- $(M_H)^2 \approx L \cdot (m_h)^2 \approx L \cdot L^{-1} \langle\Phi\rangle^2$

$$M_H = K \langle\Phi\rangle$$ (K being a Λ – independent constant

Checking the logarithmic trend on the lattice means to find a constant c_2 such that

$$(M_H)^2 = L \cdot (m_h)^2 \cdot (c_2)^{-1}$$

Then from $(m_h)^2 = (\lambda/3) \langle\Phi\rangle^2$ and $\lambda \approx (16 \pi^2 /3 L)$

we find $$K = (4 \pi/3) (c_2)^{-1/2}$$

Estimating M_H from lattice simulations

Table 5: The values of $M_{\rm H}$, as obtained from a direct fit to the higher-momentum propagator data. The two entries at $\kappa = 0.0749$, from our new simulations on a 76^4 lattice, refer to higher-momentum fits for $\hat{p}^2 > 0.1$ and $\hat{p}^2 > 0.2$ respectively. In the last column we report the combination $(c_2)^{-1/2} \equiv M_H \cdot (m_h)^{-1} \cdot [\ln(\Lambda_s/m_{\rm M_H})]^{-1/2}$.

κ	$M_{\rm H}$	$(m_h)^{-1}$	$[\ln(\Lambda_s/{\rm M_H})]^{-1/2}$	$(c_2)^{-1/2}$
0.07512	0.2062(41)	5.386(23)	0.606(2)	0.673(14)
0.0751	~ 0.200	5.568(16)	~ 0.603	~ 0.671
0.07504	0.1723(34)	6.636(32)	0.587(2)	0.671(14)
0.0749	0.0933(28)	13.00(14)	0.533(2)	0.647(20)
0.0749	0.100(6)	13.00(14)	0.538(4)	0.699(42)

- **$(c_2)^{-1/2} = 0.67 \pm 0.01$ (stat) ± 0.02 (sys)**
- **$K \equiv (4/3)\pi(c_2)^{-1/2} = 2.81 \pm 0.04$ (stat) ± 0.08 (sys)**
- **$M_H = K \langle\Phi\rangle = 690 \pm 10$ (stat) ± 20 (sys) GeV**

Recovering the traditional upper bound on m_h

- The basic relations of our picture are $L \approx \ln(\Lambda/\langle\Phi\rangle)$

$$\lambda \sim L^{-1} \qquad m_h^2 \sim \langle\Phi\rangle^2 \cdot L^{-1} \qquad M_H^2 \sim L \cdot m_h^2 = K^2 \langle\Phi\rangle^2 \quad (2)$$

- From the third relation in (2) we deduce $m_h \ll M_H$ for a large L. But M_H is cutoff independent. Therefore, by decreasing L, M_H remains fixed but m_h increases by approaching its maximum value $\mathbf{(m_h)^{max} \approx M_H}$ for L~1, i.e. for small cutoff Λ which is a few times M_H. In this limit, only one very broad resonance.
- Note that this maximum value of m_h corresponds to

our picture → $(m_h)^{\rm max} \sim (M_H)^{\rm Theor} = 690 \pm 10\ ({\rm stat}) \pm 20\ ({\rm sys})\ {\rm GeV}$

in good agreement with the traditional upper bound obtained in the past from the first two relations in Eq.(2)

traditional estimate → $(m_h)^{\rm max} = 670\ (80)\ {\rm GeV},$

See Lang's complete review arXiv:hep-lat/9312004

- Viceversa, without performing our lattice simulations, we could have predicted $\mathbf{(M_H)^{Theor} = 670\ (80)\ GeV}$ by combining the cutoff independence of M_H , the third relation in Eq.(2) and Lang's estimate of $\mathbf{(m_h)^{max}}$

Basic phenomenology of the heavy resonance

- A Higgs resonance with mass $\mathbf{M_H = K \langle\Phi\rangle \approx 700}$ **GeV** is usually believed to be a broad resonance due to strong interactions in the scalar sector
- This belief derives from two sources:

1) the definition of M_H from the quadratic shape of the potential, which is not valid in our case where $\mathbf{(m_h)^2 = V''_{eff}(\langle\Phi\rangle)}$

2) the tree-level calculation in the unitary gauge where, at asymptotic energy, due to a not complete cancelation of the graphs, the mass squared in the Higgs propagator is effectively promoted to a coupling constant $\mathbf{\lambda_0 = 3(M_H)^2/\langle\Phi\rangle^2}$

- However, at the Fermi scale $\mathbf{\mu \approx \langle\Phi\rangle}$, resumming the higher-order scalar interactions with the β-function leads to the replacement

$$\lambda_0 \rightarrow \lambda(\mu \approx \langle\Phi\rangle) = 3(m_h)^2 / \langle\Phi\rangle^2$$

This replacement expresses the **Equivalence Theorem** which holds to **all orders in the scalar self interactions and to lowest order in** $\mathbf{(g_{gauge})^2}$

- Therefore, the hypothetical second resonance, coupling to longitudinal W's with the same typical strength as the 125 GeV resonance, would be a relatively narrow resonance decaying predominantly to $\mathbf{t\bar{t}}$ quarks
- For this reason it would mainly be produced at LHC through gluon-gluon fusion

H couples to longitudinal W's with the same typical strength as the 125 GeV resonance. Therefore, as compared to their conventional values, the widths Γ(H→WW) and Γ(H→ZZ) are suppressed by the ratio $\mathbf{(m_h/M_H)^2 \approx 0.032}$ and thus are much smaller than conventionally. However, there are new processes

- H→ hh **h=h(125)**
- H→hhh, H→hWW, H→hZZ…
- Due to H-h overlapping, it is difficult to estimate precisely the total width Γ(H→all). Spectral density in the Higgs propagator is not simply the sum of two δ-functions
- However from **ATLAS & CMS ($b\bar{b}$+γγ)** channel, we find **B(H→hh) ‹ 0.12÷0.15** at the **95%** so that we expect **Γ(H→all) ≈ 30 ÷ 40 GeV**
- In conclusion, signatures of the second Higgs resonance:

i) mass around 700 GeV

ii) produced at LHC mainly through gluon-gluon fusion

iii) total width 30 ÷ 40 GeV

• Search for experimental signals in the LHC data

- A very large branching ratio $B(H \to t\bar{t}) \approx 75\%$ is expected
- However, in the relevant range of invariant mass $m(t\bar{t}) \approx 700$ GeV, the cross section $\sigma(gg \to H \to t\bar{t}) \approx 0.75$ pb would be about **100 times smaller than the background:**
- **CMS:** JHEP 02 (2019) 149 ; arXiv:1811.06625v2 [hep-ex]

Table 12: The measured differential cross section and bin boundaries for each bin of the normalized and absolute measurements of the $t\bar{t}$ differential cross section at parton level in the full phase space as a function of $m_{t\bar{t}}$ are tabulated.

$m_{t\bar{t}}$ [GeV]	$\frac{1}{\sigma}\frac{d\sigma}{dm_{t\bar{t}}}$ [GeV $^{-1}$]	$\frac{d\sigma}{dm_{t\bar{t}}}$ [pb/GeV]	
[300, 380]	$(1.981 \pm 0.036 \pm 0.18) \times 10^{-3}$	$1.664 \pm 0.031 \pm 0.163$	
[380, 470]	$(3.992 \pm 0.049 \pm 0.183) \times 10^{-3}$	$3.354 \pm 0.041 \pm 0.324$	
[470, 620]	$(2.009 \pm 0.023 \pm 0.057) \times 10^{-3}$	$1.688 \pm 0.019 \pm 0.122$	
[620, 820]	$(6.363 \pm 0.108 \pm 0.355) \times 10^{-4}$	$0.535 \pm 0.009 \pm 0.038$	← **$\sigma \approx 107 \pm 7.6$ pb**
[820, 1100]	$(1.438 \pm 0.041 \pm 0.105) \times 10^{-4}$	$0.121 \pm 0.003 \pm 0.012$	
[1100, 1500]	$(2.72 \pm 0.106 \pm 0.206) \times 10^{-5}$	$(2.285 \pm 0.089 \pm 0.21) \times 10^{-2}$	
[1500, 2500]	$(2.45 \pm 0.24 \pm 0.464) \times 10^{-6}$	$(2.059 \pm 0.201 \pm 0.383) \times 10^{-3}$	

- Dropping H → $t\bar{t}$ we have considered the following channels:

- 1) **ATLAS charged 4-lepton** events for **m(4l) = 530 ÷830 GeV**
- 2) **ATLAS γγ** events for invariant mass **m(γγ) = 600 ÷770 GeV**
- 3) **ATLAS & CMS ($b\bar{b}$ + γγ)** final state
- 4**) CMS γγ** events produced in **pp double-diffractive scattering**

The process H→ 4 charged leptons

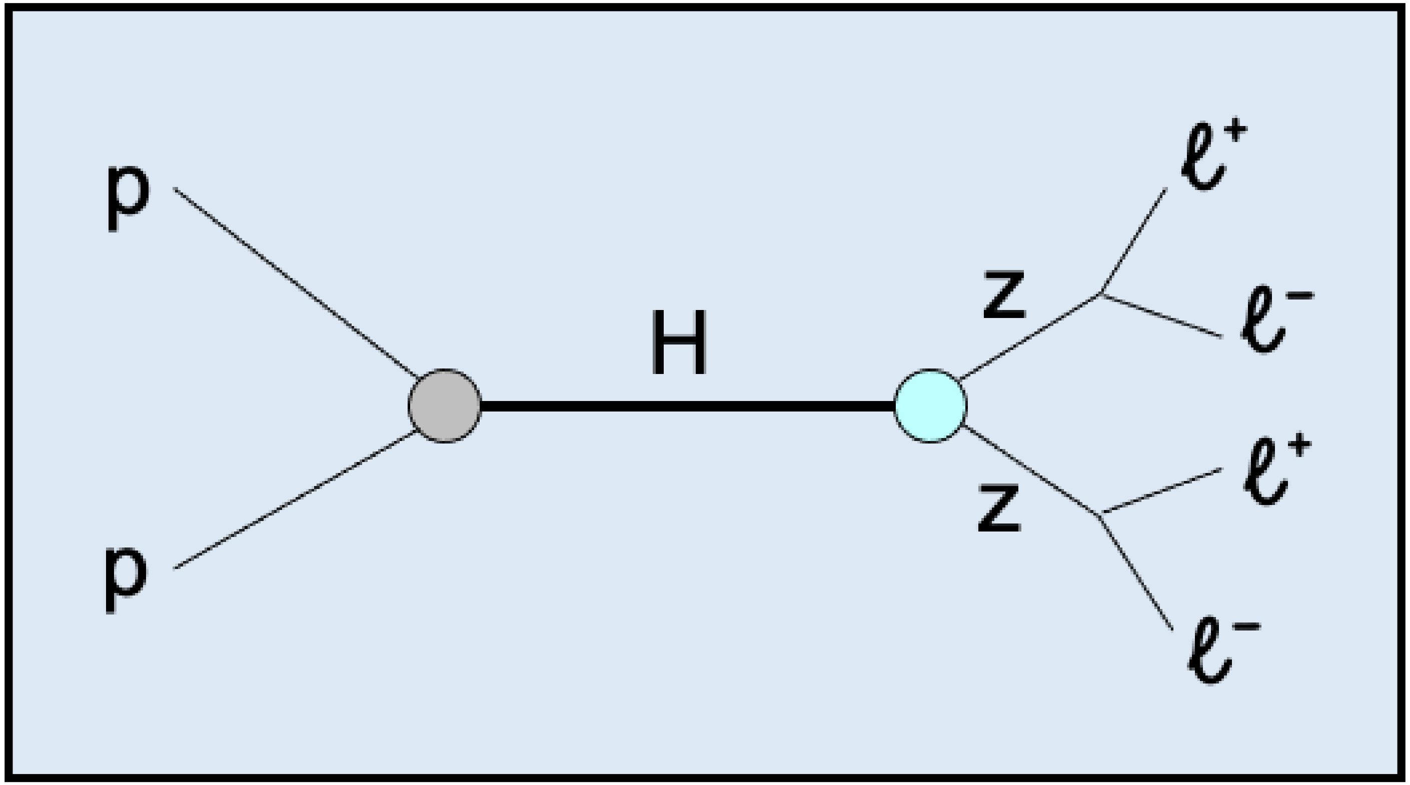

ATLAS full 4-lepton cross-section m_{4l} = 530÷830 GeV

see Fig.5 of JHEP 07(2021)005; arXiv:2103.01918v1 [hep-ex]

Large 60 GeV bins to reduce spurious migration of events between adjacent bins. For **m(4L)≈700 GeV**, resolution **Δ ≈12 GeV for 4e, 19 GeV for 2e2μ, 24 GeV for 4μ**

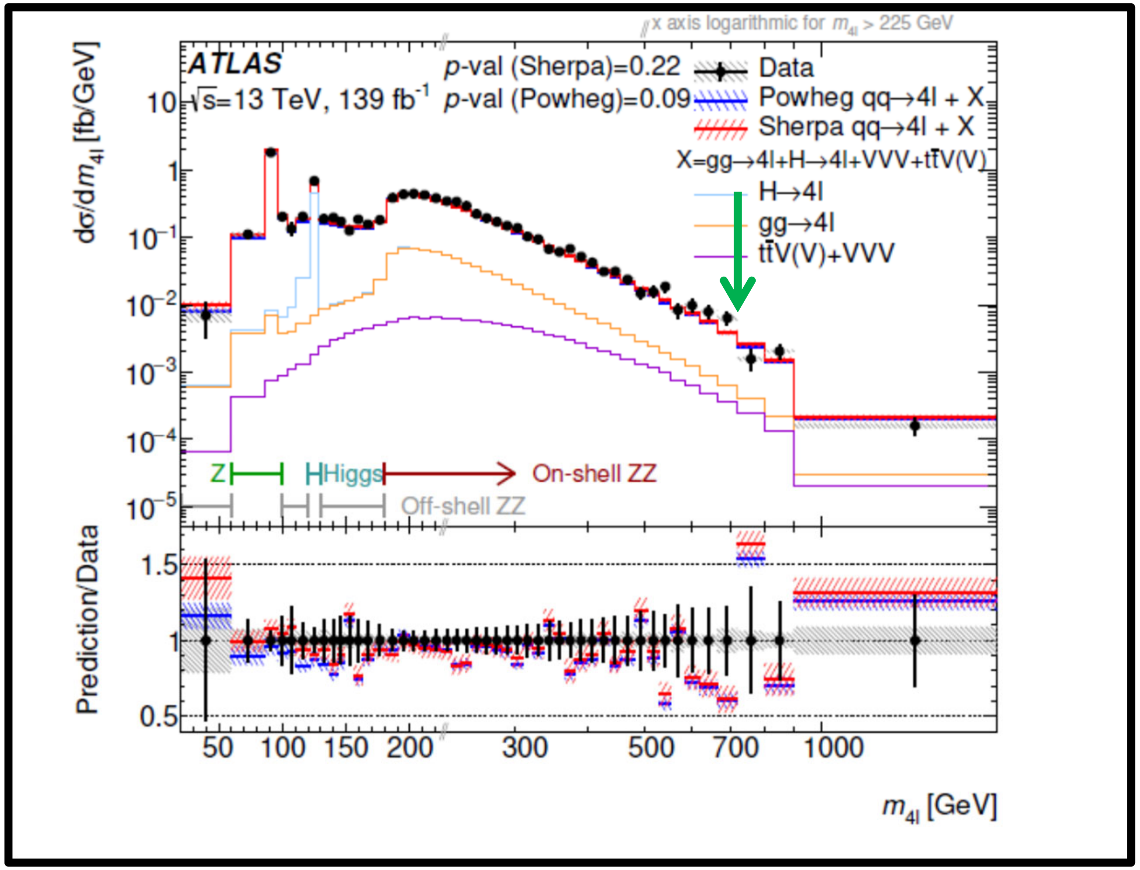

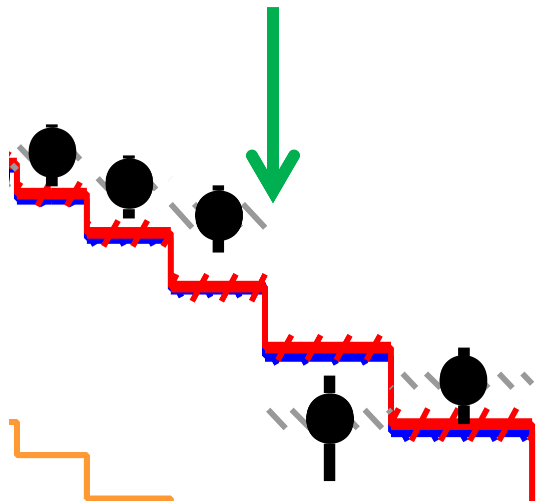

Let us consider the gluon-gluon-Fusion **(ggF) production mode**. The only set which is homogeneous and has enough statistics is the so called **ggF-low category** of events. This set provides a definite basis to understand the pattern observed in the cross section (Observed events and est. background from https://www.hepdata.net/record/ins1820316)

Table 1. For luminosity 139 fb^{-1}, we report the observed ATLAS ggF-low events and the corresponding estimated background[20] in the range of invariant mass $M_{4l} = E = 530 \div 830$ GeV. To avoid spurious fluctuations, due to migration of events between neighbouring bins, we have followed the same criterion as in Fig.5 of ref.[22] by grouping the data into larger bins of 60 GeV, centered at 560, 620, 680, 740 and 800 GeV. These were obtained by combining the corresponding 10 bins of 30 GeV, centered respectively at the neighbouring pairs: 545(15)÷ 575(15) GeV, 605(15)÷ 635(15) GeV, 665(15) ÷ 695(15), 725(15)÷755(15) GeV and 785(15)÷ 815(15) GeV as reported in ref.[20] In this energy range, the errors in the background are below 5% and will be ignored.

E[GeV]	$N_{EXP}(E)$	$N_{bkg}(E)$	$N_{EXP}(E) - N_{bkg}(E)$
560(30)	38±6.16	32.0	6.00 ± 6.16
620(30)	25±5.00	20.0	5.00 ± 5.00
680(30)	26±5.10	13.04	→ 12.96 ± 5.10
740(30)	3±1.73	8.71	→ −5.71 ± 1.73
800(30)	7±2.64	5.97	1.03 ± 2.64

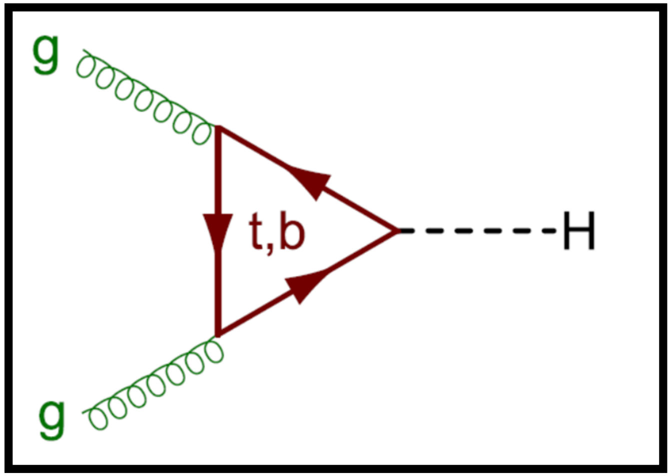

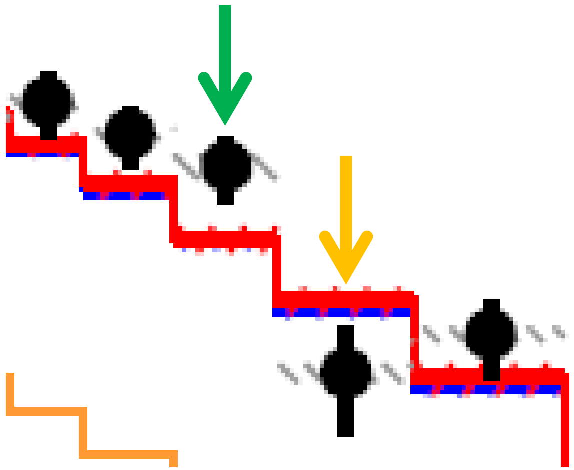

Interpretation

- ATLAS 4-lepton ggF events indicate a (+2.5σ) excess in the bin 680(30) GeV followed by an opposite (-3.3σ) defect at 740(30) GeV

- Simplest interpretation: a resonance with a mass $M_H \approx 700$ GeV, produced via the ggF mechanism, which interferes with a background and, above the Breit-Wigner peak, produces a defect of events due to the negative $(M^2_H - s)$ effect

Phenomenology in the 4-lepton channel

- For $M_H \approx 700$ GeV conventional $\Gamma(H\rightarrow ZZ)$ width is $G_F M^3_H \approx 50.1$ GeV while here

$$\Gamma(H \to ZZ) \sim \frac{M_H}{700\ \text{GeV}} \cdot \frac{m_h^2}{(700\ \text{GeV})^2}\ 50.1\ \text{GeV} \sim \frac{M_H}{700\ \text{GeV}} \cdot\ 1.6\ \text{GeV} \qquad (6)$$

$$\Gamma(H \to WW) \sim \frac{M_H}{700\ \text{GeV}} \cdot \frac{m_h^2}{(700\ \text{GeV})^2}\ 102.6\ \text{GeV} \sim \frac{M_H}{700\ \text{GeV}} \cdot\ 3.3\ \text{GeV} \qquad (7)$$

Therefore, by defining $\gamma_H = \Gamma_H/M_H$, we find a fraction

$$B(H \to ZZ) = \frac{\Gamma(H \to ZZ)}{\Gamma_H} \sim \frac{1}{\gamma_H} \cdot \frac{50.1}{700} \cdot \frac{m_h^2}{(700\ \text{GeV})^2} \sim \frac{0.0023}{\gamma_H} \qquad (9)$$

that will be replaced in the cross section approximated by on-shell branching ratios

$$\sigma_R(pp \to H \to 4l) \sim \sigma(pp \to H) \cdot B(H \to ZZ) \cdot 4B^2(Z \to l^+l^-) \qquad (10)$$

This should be a good approximation for a relatively narrow resonance so that one predicts a particular correlation

$$\gamma_H \cdot \sigma_R(pp \to H \to 4l) \sim \sigma(pp \to H) \cdot 10^{-5} \qquad (11)$$

which can be compared with the LHC data.

- For $M_H = 660 \div 700$ GeV one has $\sigma^{ggF}(pp \rightarrow H) \approx 920 \div 1260$ fb

- Therefore, in terms of $\gamma_H = (\Gamma_H / M_H)$, we predict a very precise correlation. The only uncertainty comes from $\sigma^{ggF}(pp \rightarrow H)$

- $[\gamma_H \cdot \sigma_R (gg \rightarrow H \rightarrow 4l)]^{Theor} \approx 0.013$ fb $\qquad M_H = 660$ GeV

- $[\gamma_H \cdot \sigma_R (gg \rightarrow H \rightarrow 4l)]^{Theor} \approx 0.009$ fb $\qquad M_H = 700$ GeV

or

- $[\gamma_H \cdot \sigma_R (gg \rightarrow H \rightarrow 4l)]^{Theor} \approx (0.011 \pm 0.002)$ fb

Background + resonance explain the excess and defect in the data

Table 2. The experimental ATLAS ggF-low events are compared with our theoretical prediction Eq.(14) for $M_H = 706$ GeV, $\gamma_H = 0.041$, $P = 0.14$.

E[GeV]	$N_{EXP}(E)$	$N_{TH}(E)$	χ^2
560(30)	38±6.16	36.72	0.04
620(30)	25±5.00	25.66	0.02
680(30)	26±5.10	26.32	0.00
740(30)	3±1.73	3.23	0.02
800(30)	7±2.64	3.87	1.40

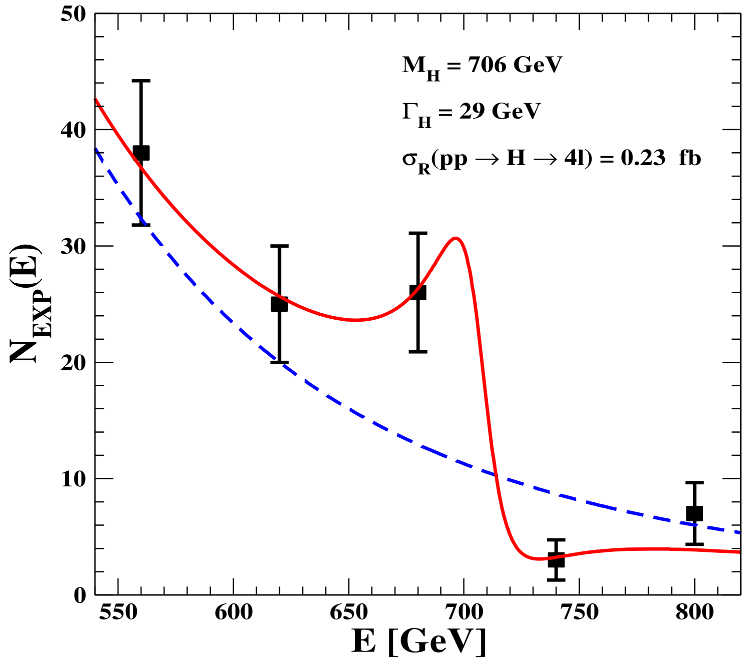

- **Red line = background + resonance** **M_H =706(25) GeV and Γ_H = 29(20) GeV**
- **Blue dashed line = ATLAS background only**
- Results of the fit have large errors γ_H **≈ 0.041 ± 0.029** **σ_R ≈ 0.23 ± 0.10 fb**
- But central values give $\langle\gamma_H\rangle \cdot \langle\sigma_R\rangle$ **≈ 0.009 fb** in excellent agreement with

$[\gamma_H \cdot \sigma_R\,(gg \to H \to 4l)]^{Theor} \approx$ 0.009 fb **M_H = 700 GeV**

Other signals in the same mass region

- i) ATLAS high-mass $\gamma\gamma$ events

- ii) ATLAS & CMS search for a new X through the chain

  $pp \rightarrow X \rightarrow h(125) + h(125) \rightarrow (b\bar{b} + \gamma\gamma\ )$

- iii) CMS search for high mass $\gamma\gamma$ pairs produced in pp double-diffractive scattering

  $pp \rightarrow p + X + p$

  and then **$X \rightarrow \gamma\gamma + \ldots$**

ATLAS γγ spectrum: a (local) 3.3 σ excess at E=684 GeV

see ATLAS Coll. PLB 822 (2021) 136651

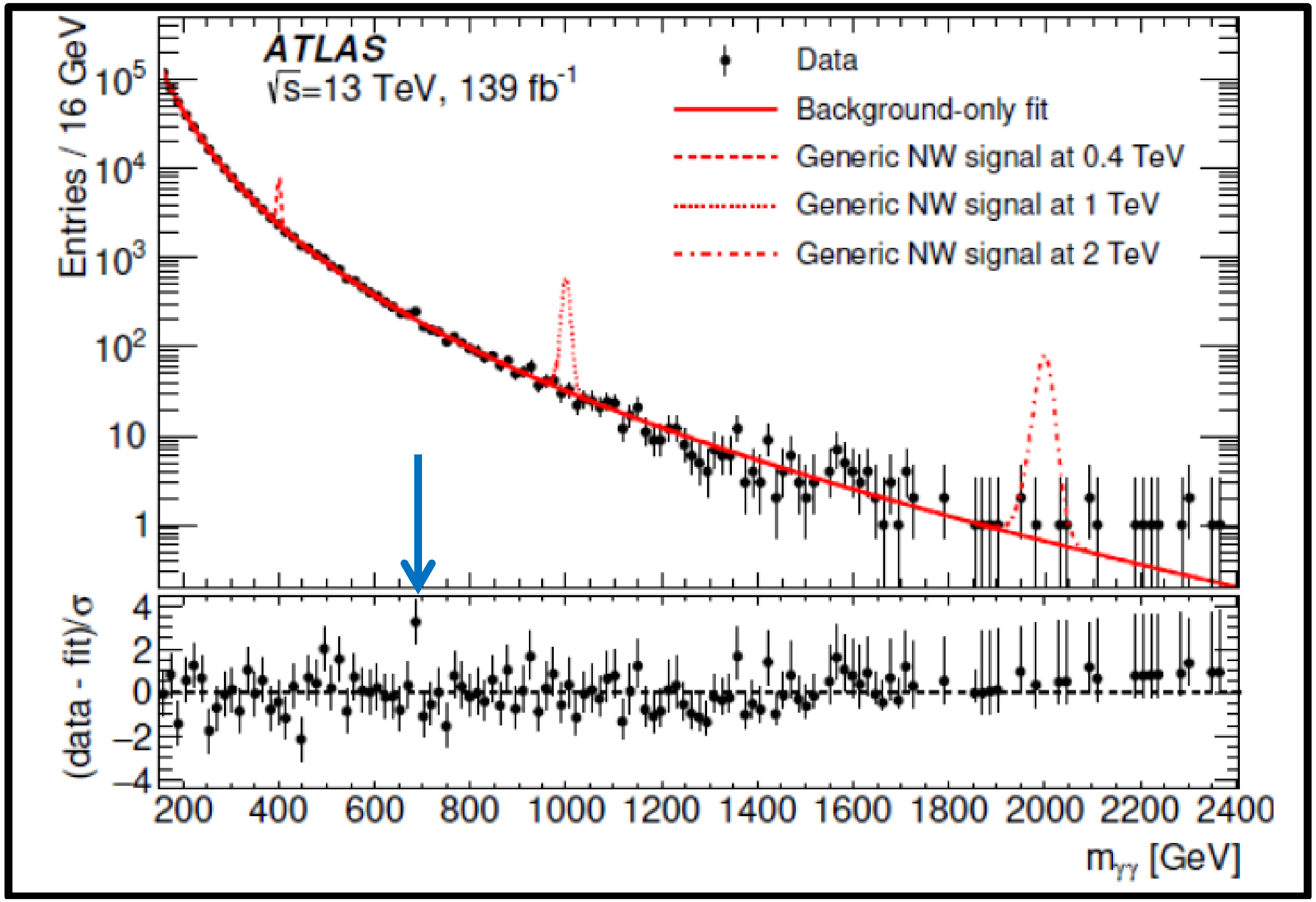

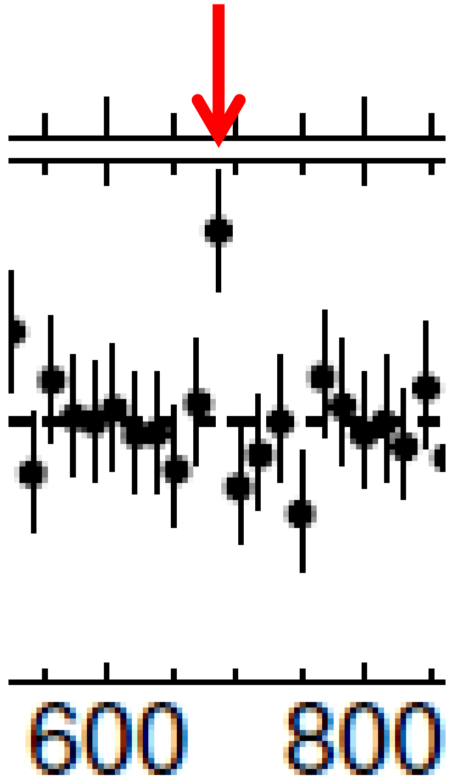

Fit to ATLAS $\gamma\gamma$ with background only ($\chi^2 = 14$)

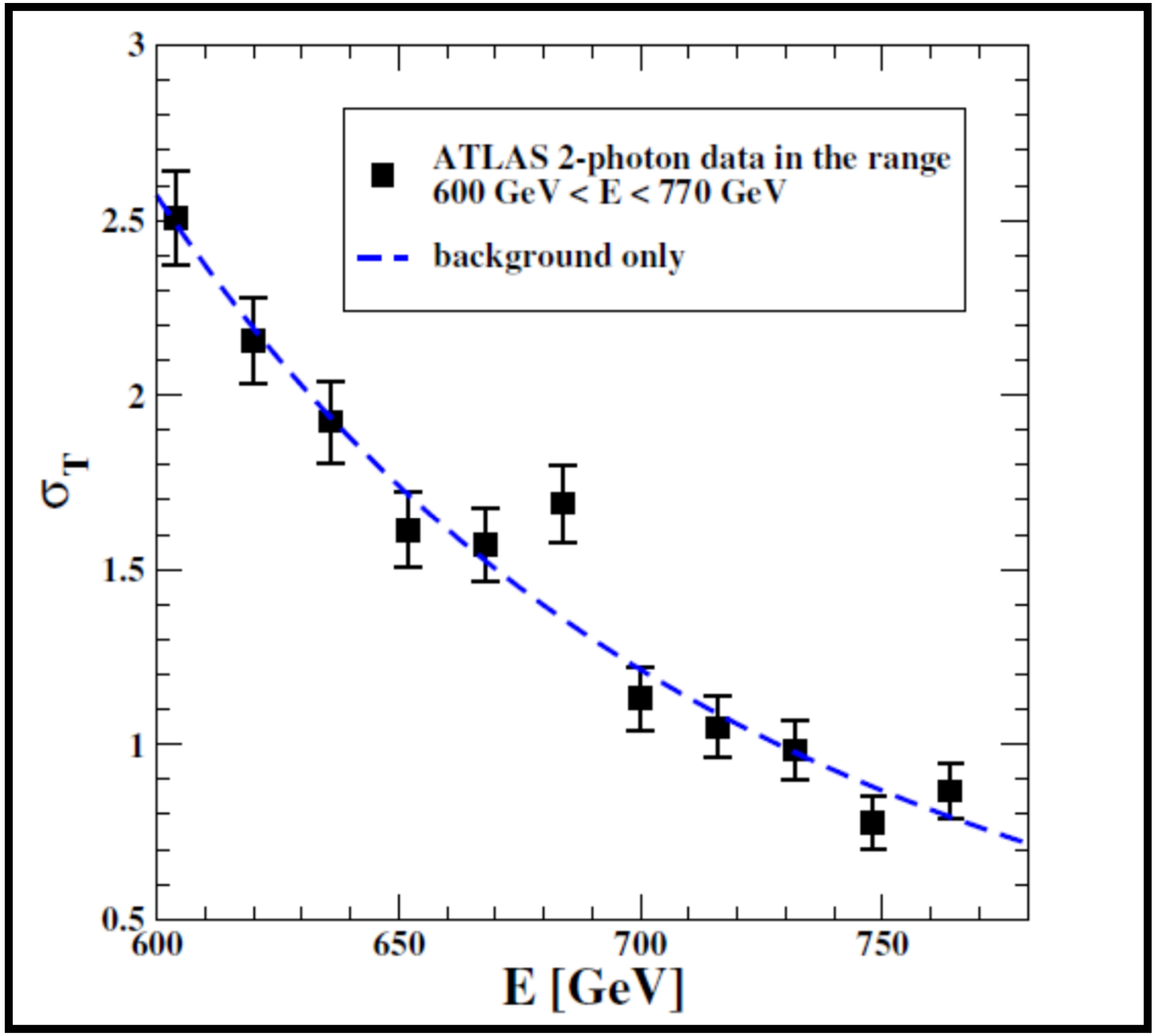

Fit to ATLAS γγ events with background + resonance

(χ^2 =7.5, 8.8, 10.2)

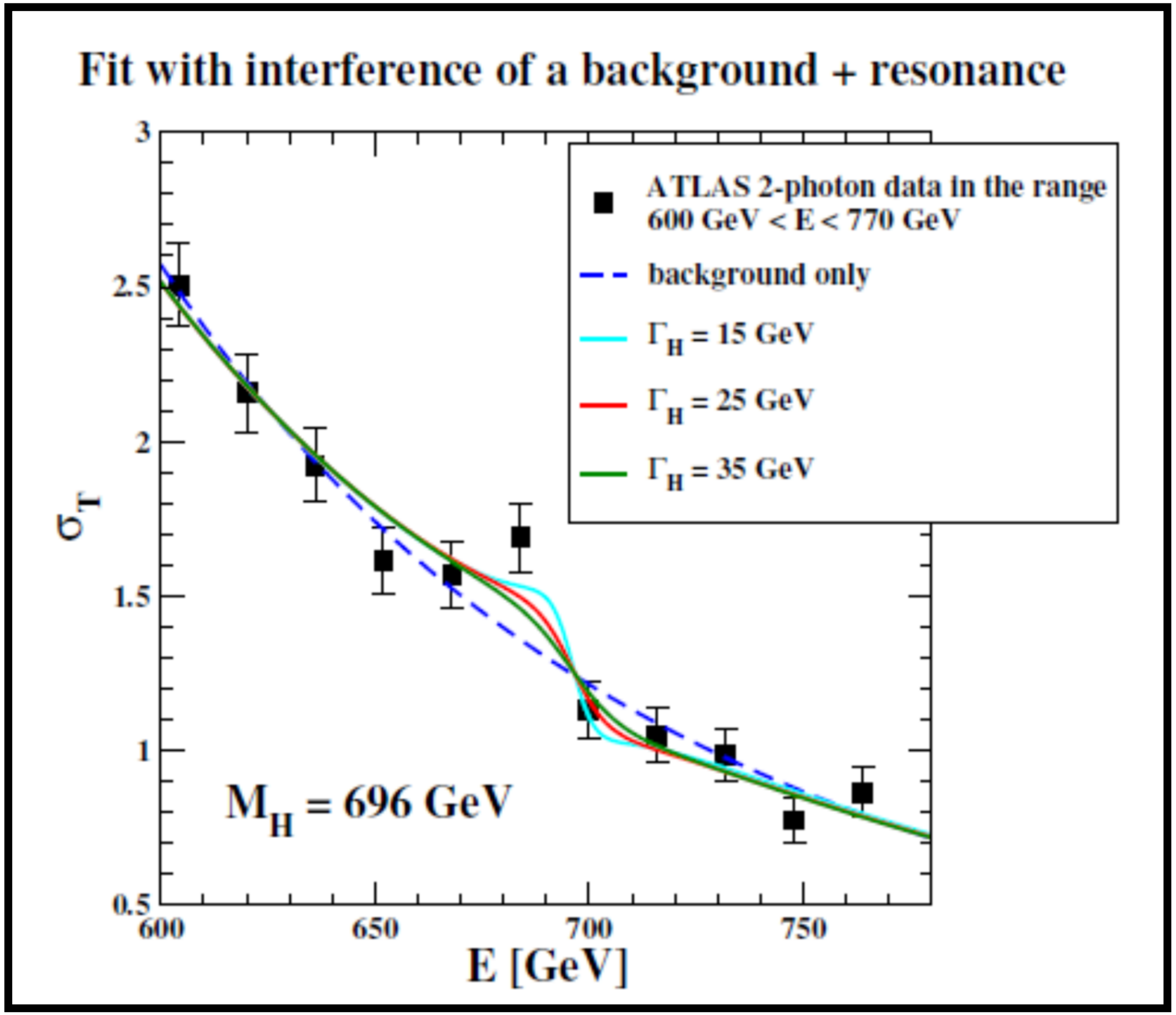

The process X=H→h(125)+h(125)→2b-quark jets + γγ

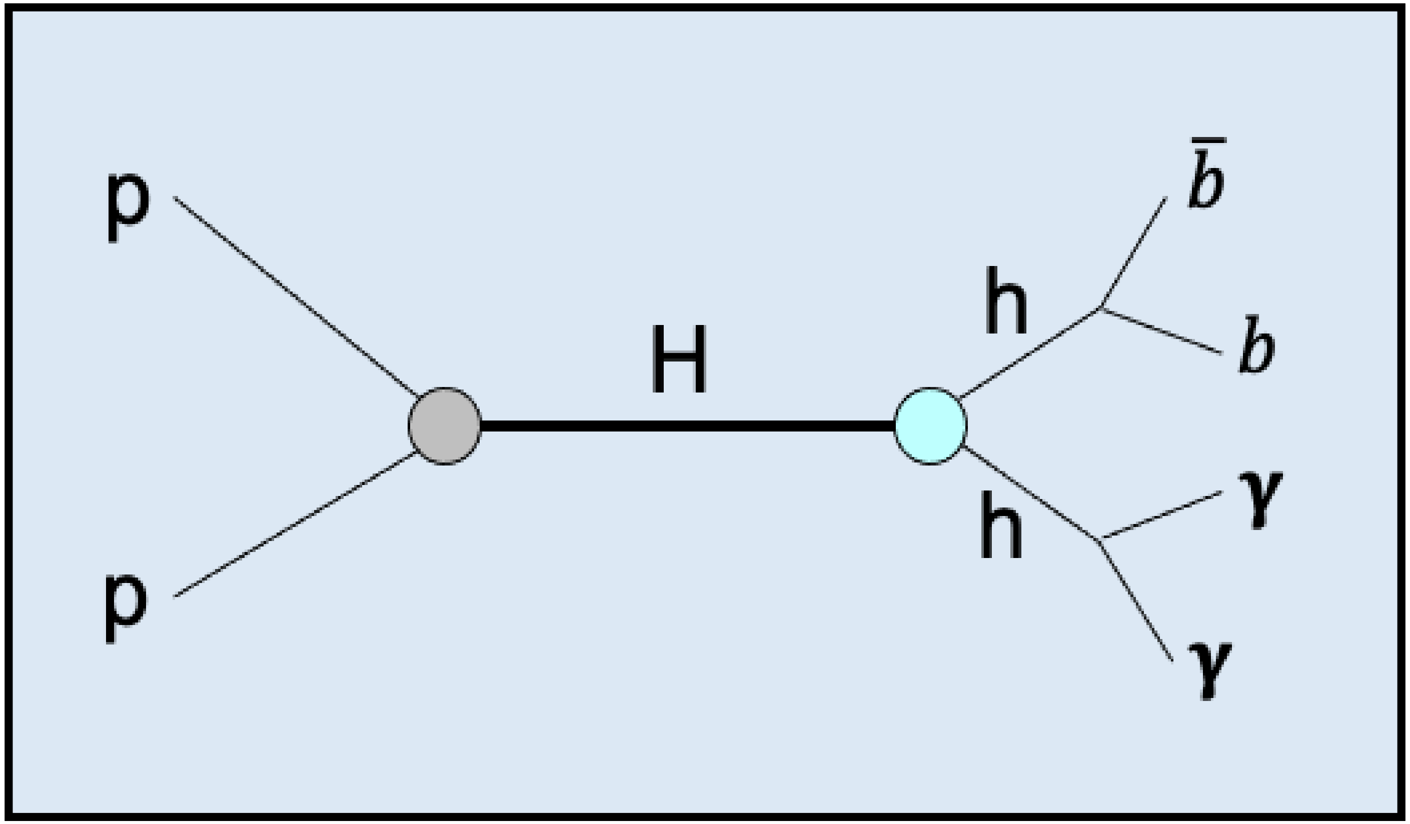

CMS analysis of the cross section for the process

pp→ X → h(125)+h(125)→ (b$\bar{b}$ +γγ) (Report CMS-PAS-HIG-21-011)

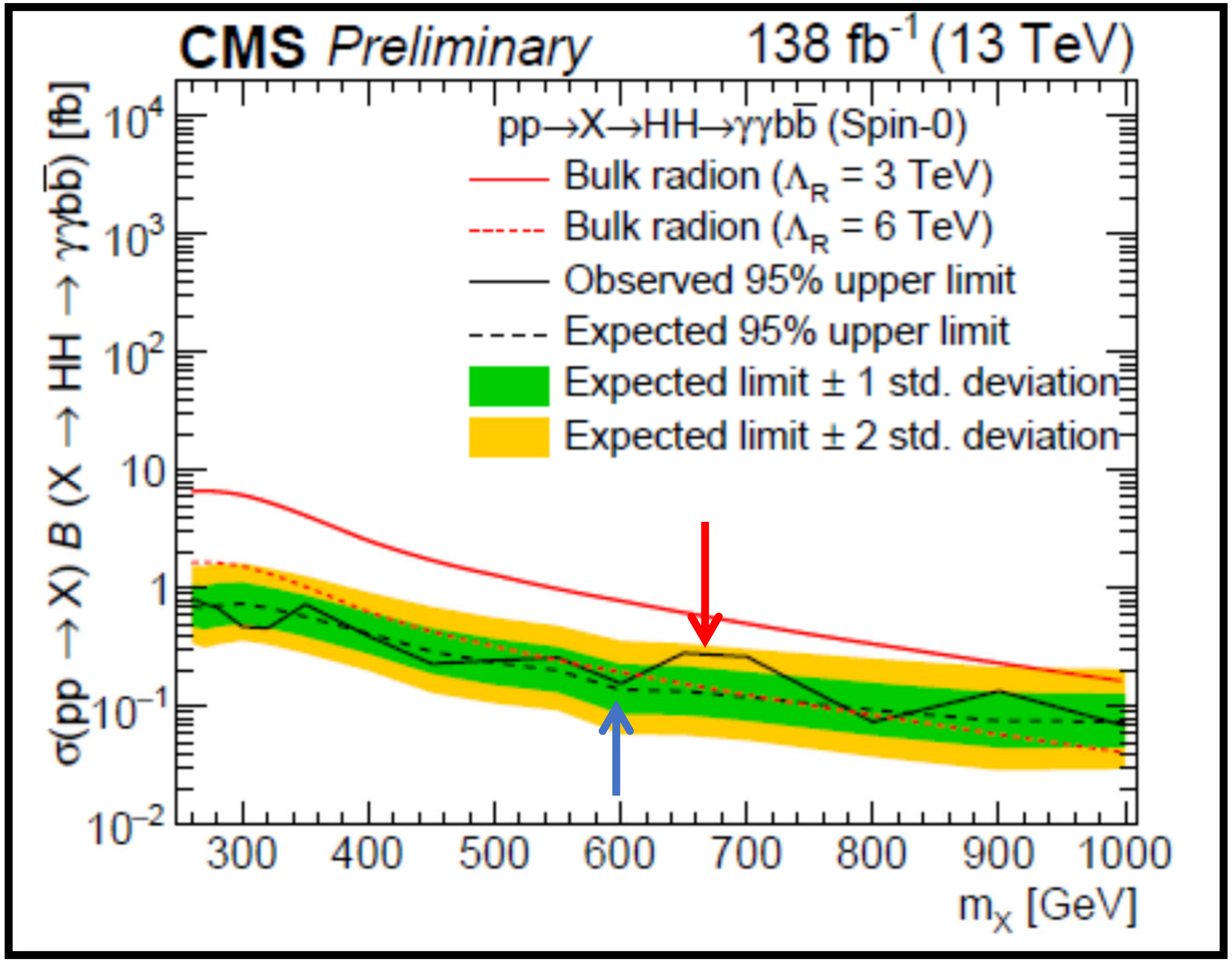

- At **600 GeV,** observed and estimated 95% CL coincide for a value **0.16 fb**
- In the **plateau 675(25) GeV**, the limit placed by the observed events is **0.30 fb**, about twice the expected background with a **1.6 σ** excess

ATLAS limits for spin-0 X→H(125)H(125)→($b\bar{b}$+γγ)

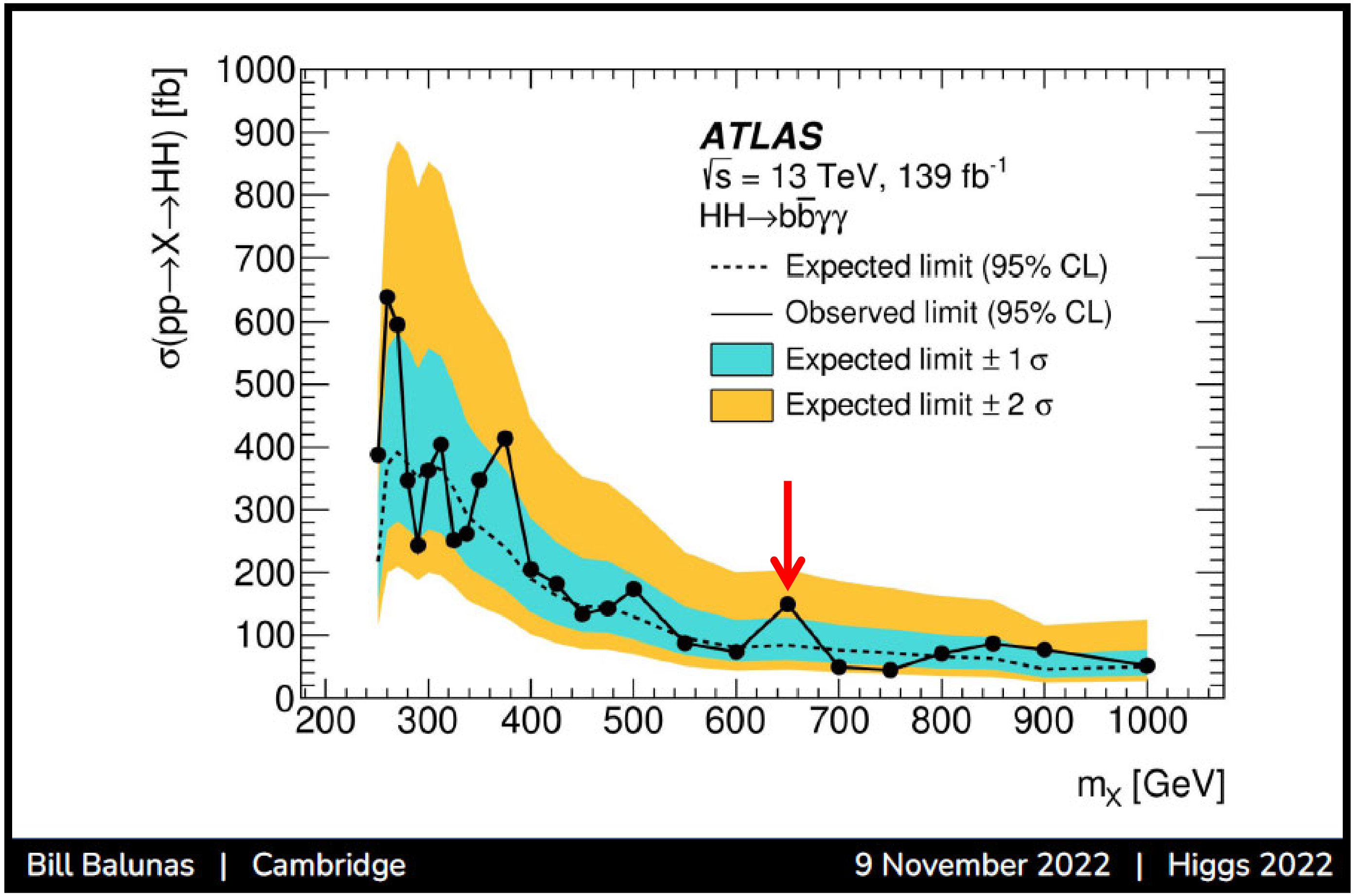

- **+1.2 σ at 650(25) GeV** compare with the +1.6 σ at 675(25) GeV by CMS. Note: soon after the excess → **-1.3 σ defect from 700 to 750 GeV**. As in ATLAS 4-leptons, this suggests again a negative interference effect after Breit-Wigner peak

Double-diffractive pp scattering producing a state X→ γγ +…
with the same quantum numbers of the vacuum

(«Diffractive excitation of the vacuum» M.Albrow, arXiv:1010.0625 [hep-ex])

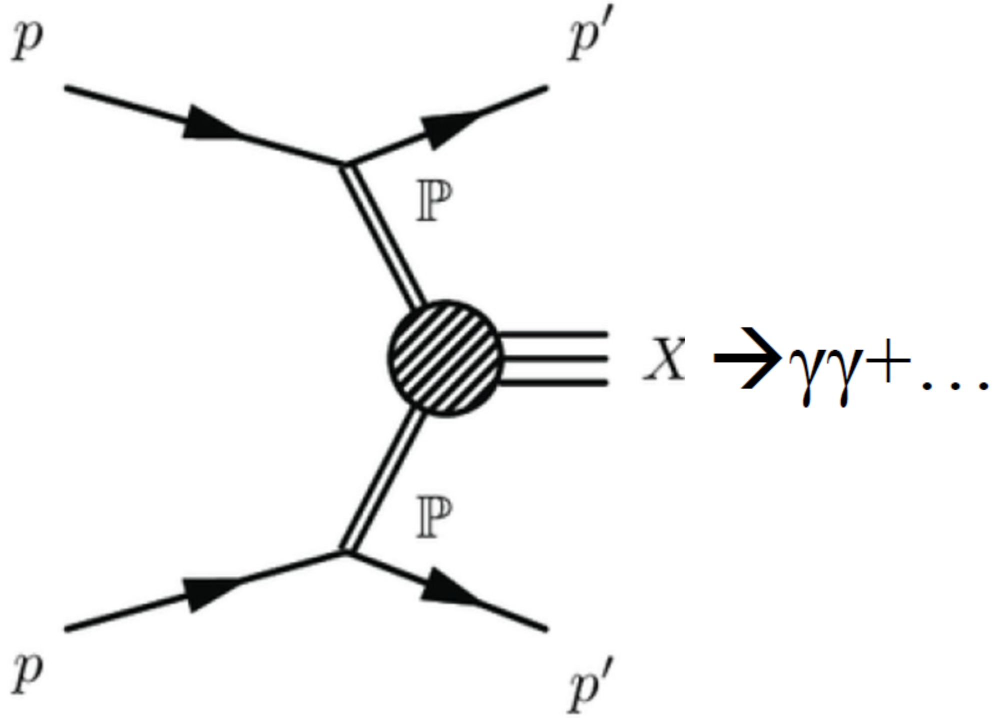

CMS analysis of γγ produced in pp double-diffractive scattering (Report CMS-TOTEM Coll. CMS-PAS-EXO-21-007)

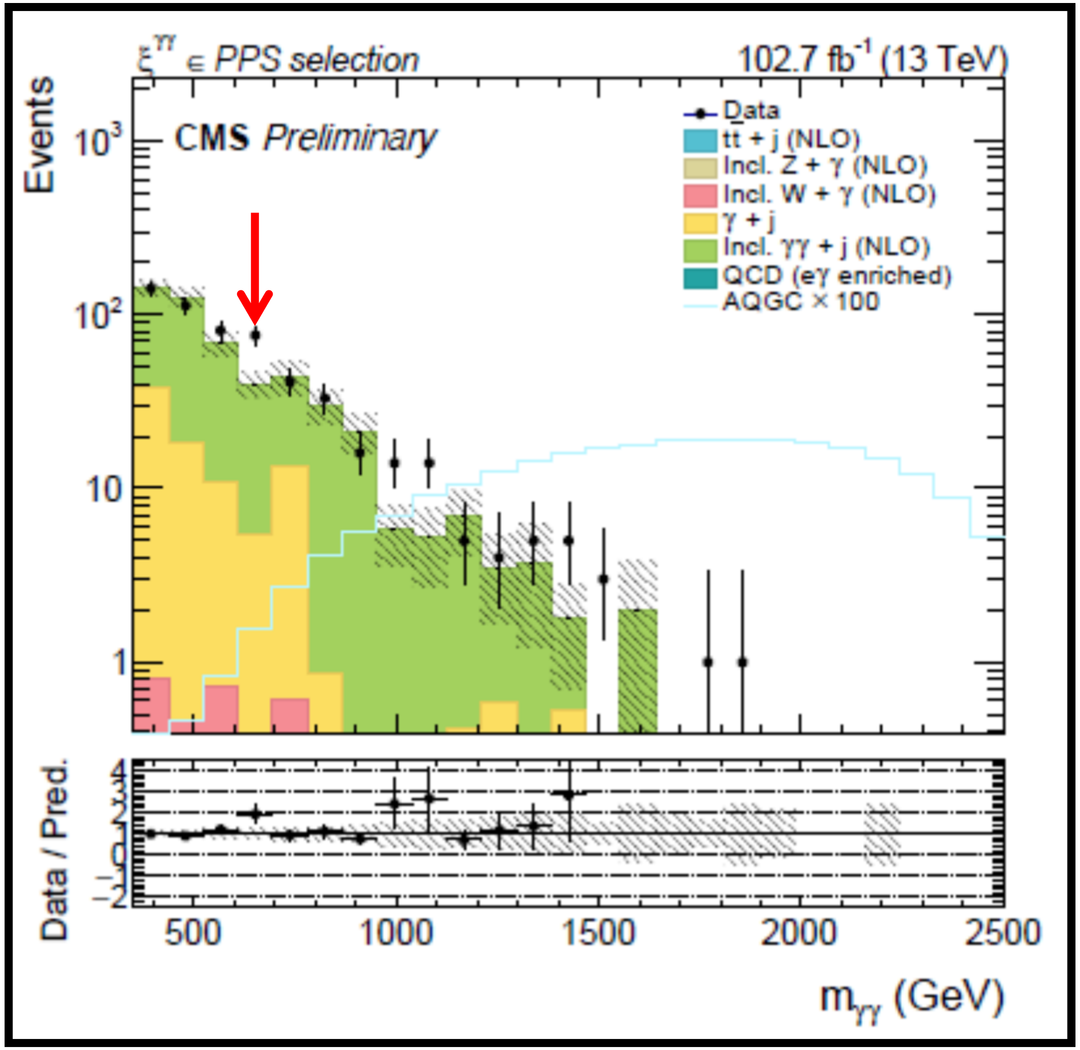

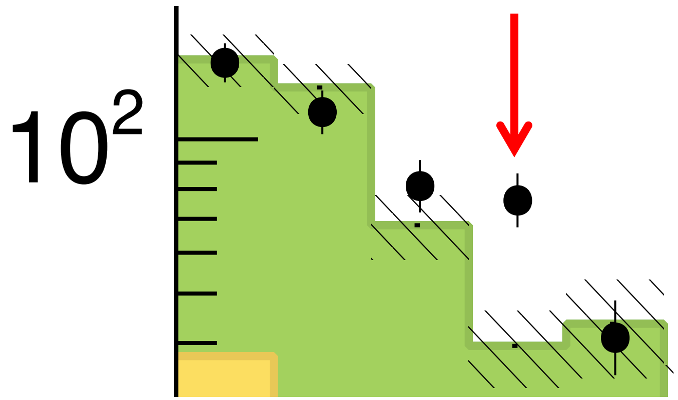

- For a m(γγ)= 650(40) GeV → 76(9) OBSERVED vs. 40(9) EXPECTED
- In the most conservative case this is a 3 σ effect (the only significant excess)

Combining the various determinations

Let us combine the determinations of $\mathbf{M_H}$ from the 5 data sets:

- $\mathbf{(M_H)^{EXP} = 706\ (25)\ GeV}$ fit to ATLAS ggF-low 4-lepton events
- $\mathbf{(M_H)^{EXP} = 696\ (13)\ GeV}$ fit to ATLAS inclusive γγ events
- $\mathbf{(M_H)^{EXP} \sim 650\ (25)\ GeV}$ excess observed in ATLAS ($b\bar{b}$+γγ) events
- $\mathbf{(M_H)^{EXP} \sim 675\ (25)\ GeV}$ excess observed in CMS ($b\bar{b}$+γγ) events
- $\mathbf{(M_H)^{EXP} \sim 650\ (40)\ GeV}$ excess in CMS γγ events produced in pp double-diffractive scattering

- $\mathbf{(M_H)^{COMB} \sim 685\ (10)\ GeV}$

compare with

- $\mathbf{(M_H)^{THEOR} = 690\ (22)\ GeV}$
- The 5 determinations are well aligned within the uncertainties and the average mass is in very good agreement with the predicted value

Combine ATLAS & CMS data for H→h(125)h(125)→($b\bar{b}$+γγ)

- From the two cross-sections   h=h(125)
- σ(pp→H→hh) ‹ 150 fb   95%   **ATLAS**   650(25) GeV
- σ(pp→H→hh) ‹ 120 fb   95%   **CMS**   675(25) GeV
- Where one expects a ggF cross section σ(gg→H) ≈ 1000 fb
- One obtains **B(H→ hh) ‹ 0.12 ÷ 0.15   at the 95%**
- And **for a mass (M_H) ^{THEOR} ≈ 690 (22) GeV**

  a total width

Γ(H→ all) = 30 ÷ 40 GeV

- **Conclusions**: to test a definite prediction **$(M_H)^{THEOR}$ = 690(22) GeV**, one should look for deviations from the background nearby. This means that local deviations from background are not downgraded by the "look elsewhere" effect
- Therefore, we are now faced with :

  i) a **2.5-σ** excess + a **3.3-σ** defect around **700 GeV** in the ATLAS 4-leptons (ggF)

  ii) a **3.3 σ** excess at **684(16) GeV** in the ATLAS γγ channel

  iii) a **1.2 σ** excess at **650(25) GeV** in the ATLAS ($b\bar{b}$+γγ) channel

  iv) a **1.6 σ** excess at **675(25) GeV** in the CMS ($b\bar{b}$+γγ) channel

  v) a **3.0 σ** excess at **650(40) GeV** in the CMS γγ produced in pp double-diffractive scattering

- The correlation of these measurements is small, so that the cumulated statistical evidence for a new resonance around 700 GeV is now at (or above) the **5 σ** level
- Of course: i) also systematic uncertainties ii) in other channels no discrepancies (with present LHC setup, second resonance is too heavy to be seen immediately in all possible channels). Remember the h(125) discovery: at the beginning no signals in $b\bar{b}$ and ττ channels → **Present situation is unstable**
- It could soon be resolved with two crucial missing samples from RUN2:

  a) full **CMS charged 4-lepton data**

  b) full **CMS inclusive high-mass γγ data**

Partial CMS 4-lepton and 2-photon samples

Partial CMS 4-lepton events 2016+2017→ (35.9+41.5) fb^{-1}

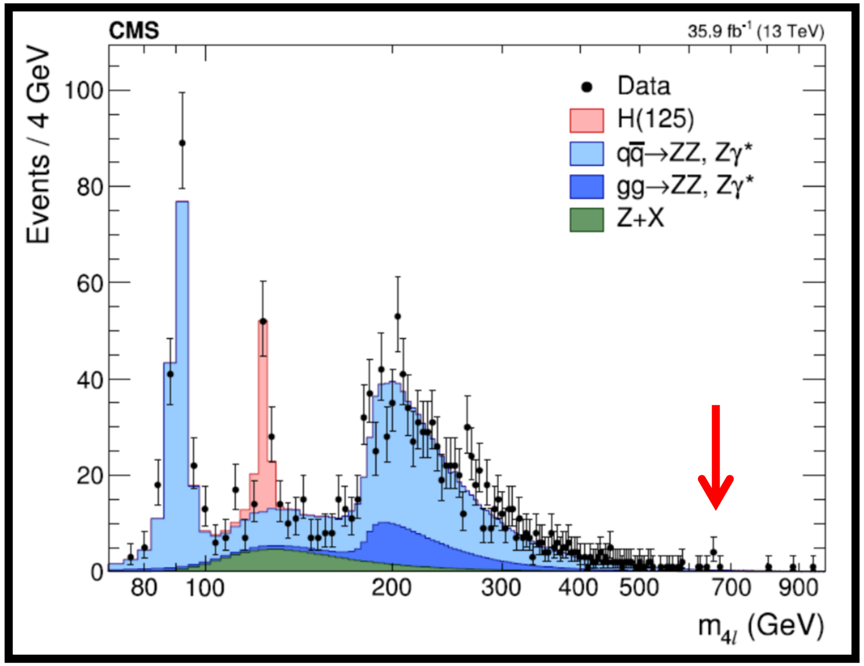

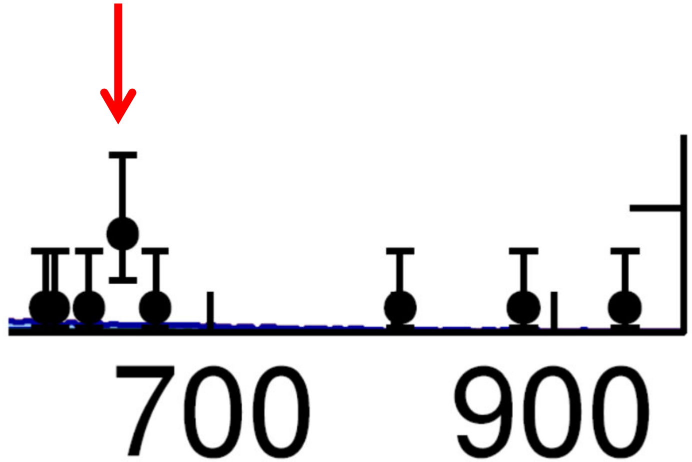

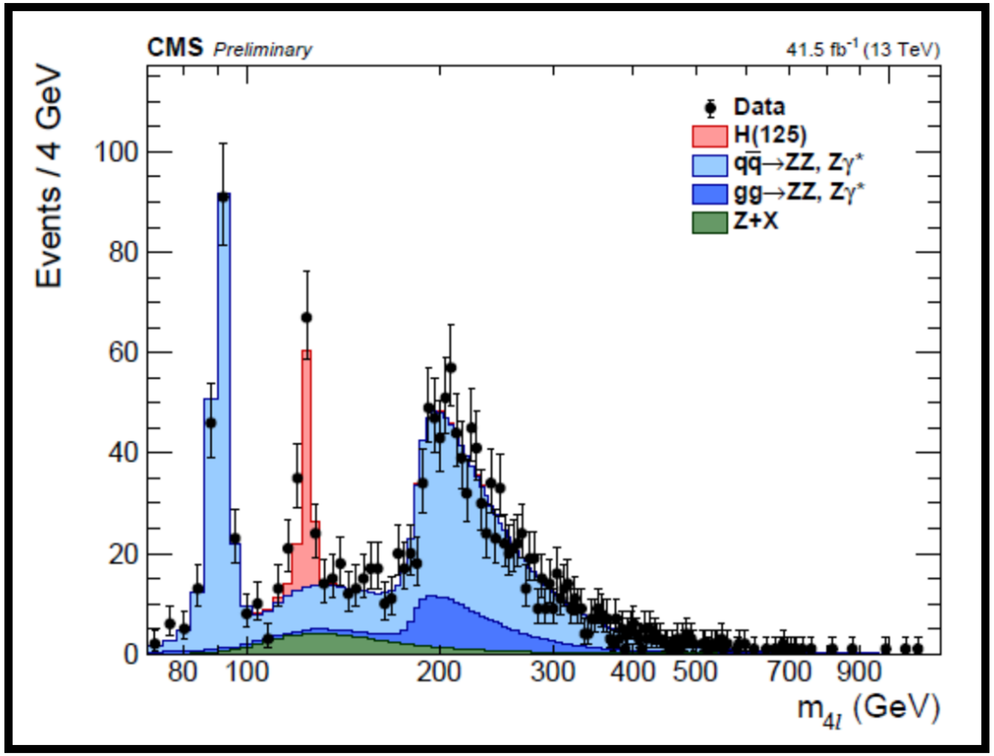

Cea’s extraction of the 2016+2017 CMS data

MPLA 34(2019)1950137

P. Cea

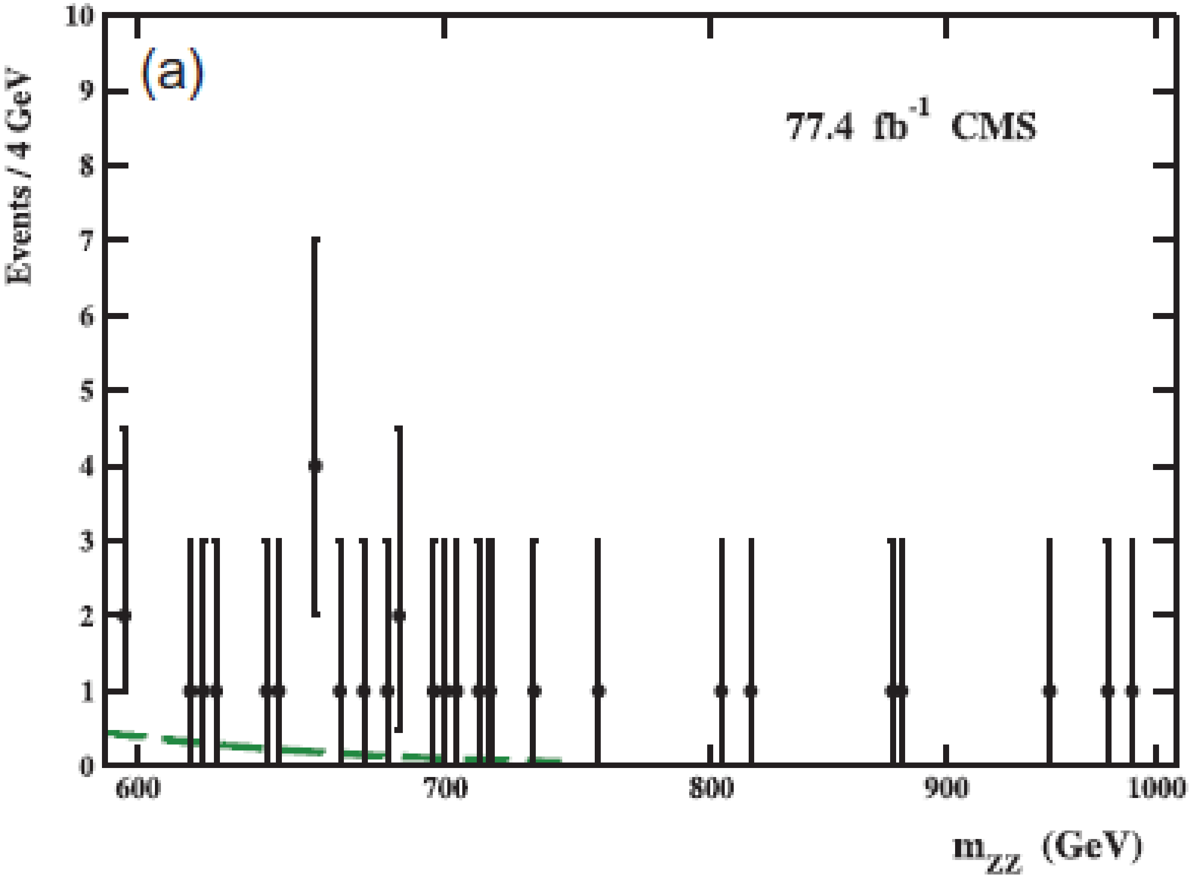

CMS: 4-lepton events E= 650÷770 GeV LUM=77.4 fb^{-1}

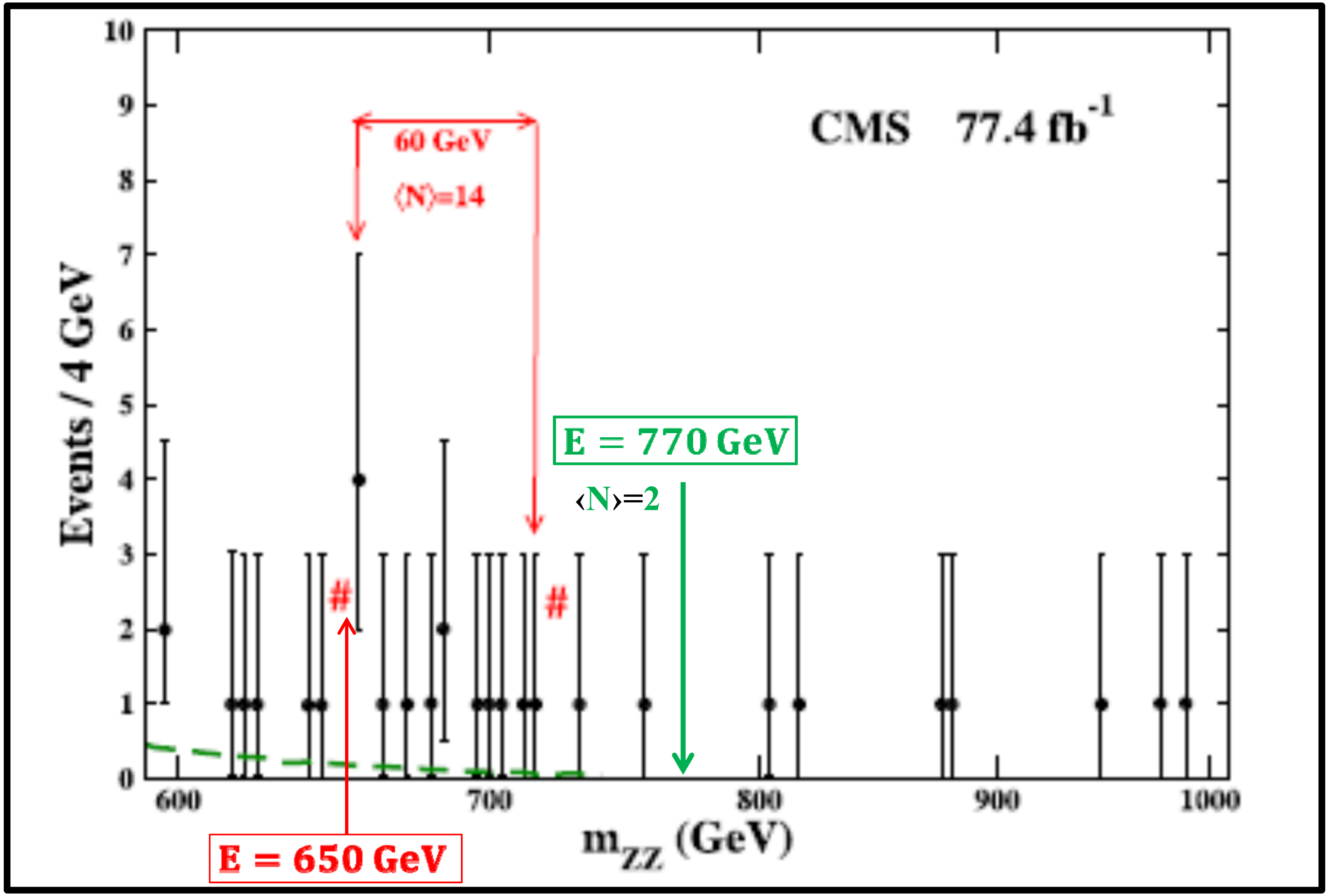

4-lepton events: CMS 77.4 $fb^{(-1)}$ vs. ATLAS 139 $fb^{(-1)}$

- **CMS 77.4 $fb^{(-1)}$ E = 650÷770 GeV → ‹N(4l)› = 14 + 2 = 16 Measured**
- **CMS 139 $fb^{(-1)}$ E = 650 ÷770 GeV → ‹N(4l)› = 28.7 (Extrapolated)**

- **ATLAS 139 $fb^{(-1)}$ E = 665(15) GeV → ‹N(4l)› = 17 Measured (*)**
  E = 695(15) GeV → ‹N(4l)› = 9 Measured (*)
  E = 725(15) GeV → ‹N(4l)› = 3 Measured (*)
  E = 755(15) GeV → ‹N(4l)› = 0 Measured (*)

ATLAS 139 $fb^{(-1)}$ E = 650÷770 GeV → ‹N(4l)› = 29 (Measured) (*)

- **(*) MVA-ggF-low category**

Low-statistics partial CMS results: inclusive γγ

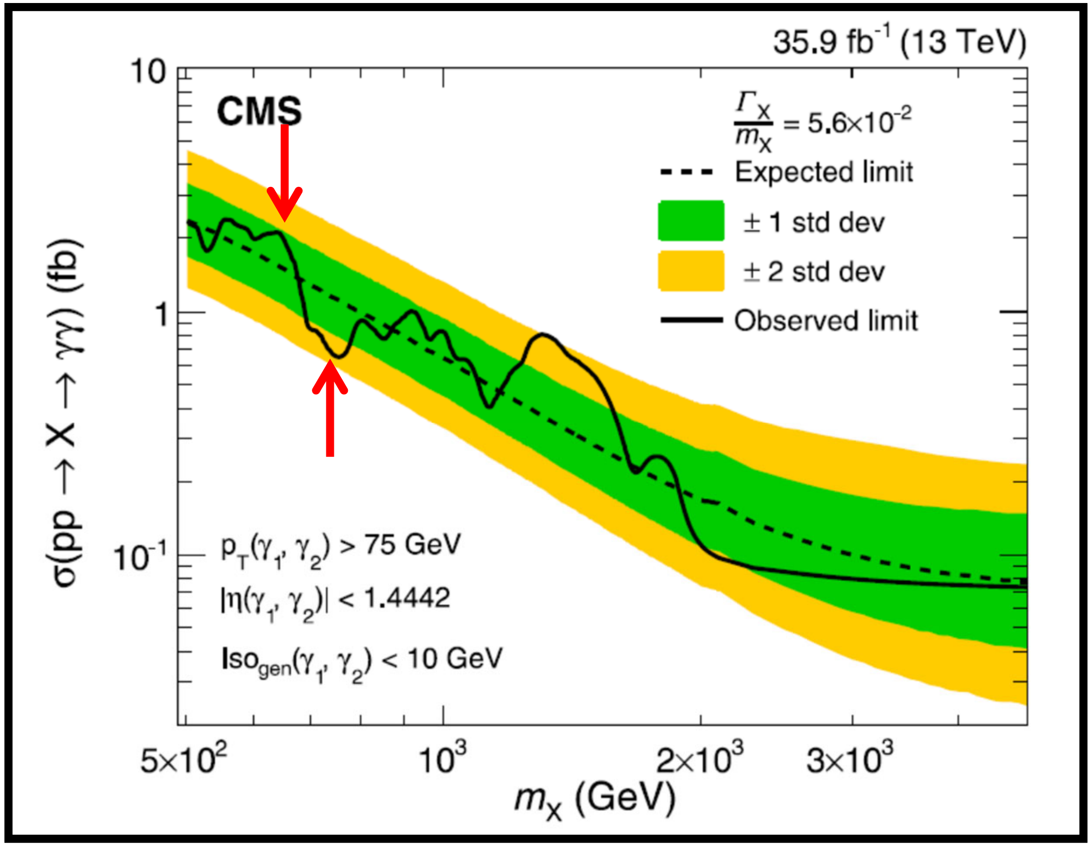

- A **1-σ excess at 640(30) GeV** followed by a **1.5-sigma defect at 750(40) GeV** (same qualitative pattern as in present ATLAS 4-leptons, with much less statistics)

Vol. 11 (2018) *Acta Physica Polonica B Proceedings Supplement* No 2

PHYSICS AFTER THE DISCOVERY OF THE HIGGS BOSON*

J.J. van der Bij

Institut für Physik, Albert-Ludwigs-Universität Freiburg, Germany

- «This said, it means that the real reason we need the Higgs field is renormalizability. This, however, does not imply that one must have a single Higgs particle peak. Fundamental quantum field theory tells us only that the Higgs field must have a Källén–Lehmann spectral density [14,15]. This density can be largely arbitrary, but must fall off fast enough at infinity, since otherwise the theory is not renormalizable. Since in some sense the Higgs field is considered to be different from other fields, it is not unreasonable to expect a non-trivial density. The premier scientific goal regarding electroweak symmetry breaking is thus to measure the Källén–Lehmann spectral density of the Higgs propagator».

A remark on radiative corrections

- With two resonances of the Higgs field, what about radiative corrections?
- Our lattice simulations indicate a propagator structure

$$G(p) \sim \frac{1 - I(p)}{2} \frac{1}{p^2 + m_h^2} + \frac{1 + I(p)}{2} \frac{1}{p^2 + M_h^2} \tag{4}$$

with an interpolating function $I(p)$ which depends on an intermediate momentum scale p_0 and tends to $+1$ for large $p^2 \gg p_0^2$ and to -1 when $p^2 \to 0$.

- This is very close to van der Bij propagator   Acta Phys. Polon. B**11** (2018) 397.

$(-1 \leq \eta \leq 1)$

$$G(p) \sim \frac{1-\eta}{2} \frac{1}{p^2 + m_h^2} + \frac{1+\eta}{2} \frac{1}{p^2 + M_H^2} \tag{49}$$

- In the ρ-parameter at one loop, this is similar to have an effective Higgs mass

$$m_{\rm eff} \sim \sqrt{m_h M_H}\, (M_H/m_h)^{\eta/2} \tag{47}$$

In our case, this would be between $m_h = 125$ GeV and $M_H \sim 700$ GeV.

- How well, the mass from radiative corrections agree with the direct LHC result 125 GeV?

From the PDG review: positive M_H-$\alpha_S(M_Z)$ correlation (Important: NuTeV is not considered → larger M_H)

Table 10.7: Values of $\hat{s}_Z^2$, s_W^2, α_s, m_t and M_H [both in GeV] for various data sets. In the fit to the LHC (Tevatron) data the α_s constraint is from the $t\bar{t}$ production [204] (inclusive jet [205]) cross-section.

Data	$\hat{s}_Z^2$	s_W^2	$\alpha_s(M_Z)$	m_t	M_H
All data	0.23122(3)	0.22332(7)	0.1187(16)	173.0 ± 0.4	125
All data except M_H	0.23107(9)	0.22310(19)	0.1190(16)	172.8 ± 0.5	90^{+17}_{-16}
All data except M_Z	0.23113(6)	0.22336(8)	0.1187(16)	172.8 ± 0.5	125
All data except M_W	0.23124(3)	0.22347(7)	0.1191(16)	172.9 ± 0.5	125
All data except m_t	0.23112(6)	0.22304(21)	0.1191(16)	176.4 ± 1.8	125
M_H, M_Z, Γ_Z, m_t	0.23125(7)	0.22351(13)	0.1209(45)	172.7 ± 0.5	125
LHC	0.23110(11)	0.22332(12)	0.1143(24)	172.4 ± 0.5	125
Tevatron + M_Z	0.23102(13)	0.22295(30)	0.1160(45)	174.3 ± 0.7	100^{+31}_{-26}
LEP	0.23138(17)	0.22343(47)	0.1221(31)	182 ± 11	274^{+376}_{-152} ←
SLD + M_Z, Γ_Z, m_t	0.23064(28)	0.22228(54)	0.1182(47)	172.7 ± 0.5	38^{+30}_{-21} ←
$A_{FB}^{(b,c)}$, M_Z, Γ_Z, m_t	0.23190(29)	0.22503(69)	0.1278(50)	172.7 ± 0.5	348^{+187}_{-124} ←
$M_{W,Z}$, $\Gamma_{W,Z}$, m_t	0.23103(12)	0.22302(25)	0.1192(42)	172.7 ± 0.5	84^{+22}_{-19} ←
low energy + $M_{H,Z}$	0.23176(94)	0.2254(35)	0.1185(19)	156 ± 29	125

First remark: NuTeV not included by PDG

The NuTeV collaboration found $s_W^2 = 0.2277 \pm 0.0016$ (for the same reference values), which was 3.0 σ higher than the SM prediction [89]. However, since then several groups have raised concerns about interpretation of the NuTeV result, which could affect the extracted $g_{L,R}^2$ (and thus s_W^2) including their uncertainties and correlation. These include the assumption of symmetric strange and antistrange sea quark distributions, the electron neutrino contamination from K_{e3} decays, isospin symmetry violation in the parton distribution functions and from QED splitting effects, nuclear shadowing effects, and a more complete treatment of EW and QCD radiative corrections. A more detailed discussion and a list of references can be found in the 2016 edition of this *Review*. The precise impact of these effects would need to be evaluated carefully by the collaboration, but in the absence of a such an effort we do not include the νDIS constraints in our default set of fits.

Second remark: the importance of $\alpha_S(M_z)$

Schmitt→ present most complete analysis

hep-ex/0401034
nuhep-exp/04-01

Apparent Excess in $e^+e^- \rightarrow$ hadrons

Michael Schmitt

Northwestern University

January 22, 2004

Abstract

We have studied measurements of the cross section for $e^+e^- \rightarrow$ hadrons for center-of-mass energies in the range 20–209 GeV. We find an apparent excess over the predictions of the Standard Model across the whole range amounting to more than 4σ.

Higgs mass from LEP1

TOKUSHIMA 95-02
(hep-ph/9503288)
March 1995

Remarks on the Value of the Higgs Mass
from the Present LEP Data

M. CONSOLI[a] AND Z. HIOKI[b]

ABSTRACT

We perform a detailed comparison of the present LEP data with the one-loop standard-model predictions. It is pointed out that for $m_t = 174$ GeV the "bulk" of the data prefers a rather large value of the Higgs mass in the range 500-1000

ALEPH+DELPHI+L3+OPAL

α_s	0.113	0.125	0.127	0.130
m_h(GeV)	100	100	500	1000
TOTAL χ^2	43.6	37.8	36.4	38.2

Table VII. Total χ^2 for the four Collaborations.

α_s	0.113	0.125	0.127	0.130
m_h(GeV)	100	100	500	1000
ALEPH	6.7	8.6	7.6	8.2
DELPHI	7.6	8.8	7.3	7.3
L3	10.3	4.7	5.4	5.9
OPAL	11.4	7.9	5.1	4.1
TOTAL χ^2	36.0	30.0	25.4	25.5

Table VIII. Total χ^2 for the four Collaborations by excluding the data for $A^o_{FB}(\tau)$.